

**Fig. 6.** Drug-induced cytotoxicity in the 3D iPSC-hepa is mediated by cytochrome P450. (A, B) The cell viability of the 3D iPSC-hepa was assessed by WST-8 assay after 24 h exposure to different concentrations of (A) Aflatoxin B1 and (B) Benzbromarone in the presence or absence of the CYP3A4 or 2C9 inhibitor, Ketoconazole or Sulfaphenazole, respectively. Cell viability was expressed as the percentage of cells treated with solvent only. \* $P < 0.05$ ; \*\* $P < 0.01$ .

hES/hiPS cell lines, it would be important to select an appropriate cell line for medical applications such as drug screening. However, the dominant reason for this hepatic differentiation propensity is not been well known. It would be interesting study to elucidate the mechanism of this propensity.

Although the drug metabolism capacity and CYP induction potency of 3D iPSC-hepa were higher than those of mono iPSC-hepa (Fig. 4B and C), they were still lower than those of primary human hepatocytes. The hepatic nuclear factors are known to be key molecules in the CYP induction of hepatocytes [30]. Therefore, overexpression of hepatic nuclear factors, which are not abundantly expressed in the hepatocyte-like cells (such as *PXR*), might upregulate the CYP induction potency of the hepatocyte-like cells.

3D iPSC-hepa were more sensitive for detection of the drug-induced cytotoxicity than HepG2 cells that are widely used to predict hepatotoxicity [31,32] (Fig. 5). In addition, the decrease of cell viability, which was caused by hepatotoxic drugs, of 3D iPSC-hepa was partially rescued by treatment with a CYP inhibitor (Fig. 6). These data suggest that the hepatocyte-like cells could detect the toxicity of the reactive metabolites that were generated by drug metabolizing enzymes such as CYP enzymes. Because in many cases, drug-induced hepatotoxicity is caused by the reactive

metabolites produced by drug metabolizing enzymes [33], our finding that the hepatocyte-like cells could detect the toxicity of reactive metabolites should be of great potential for toxicological screening. Moreover, it might be possible to predict idiosyncratic liver toxicity by using hepatocyte-like cells generated from hiPSCs that were established from a patient with a rare CYP polymorphism. However, some compounds did not show any cytotoxicity (such as Cyclizine, Felbamate, and Sulindac) (Fig. 5). To apply the hepatocyte-like cells for wide-spread drug screening, generation of the hepatocyte-like cells are required to detect hepatotoxicity in more sensitive manner. Previous studies showed that the depletion of conjugating enzymes [32] or knockdown of *Nrf2* [34] expression are useful to upregulate the sensitivity to hepatotoxic drugs. Therefore, these approaches would be useful to generate more sensitive hepatocytes to toxic drugs.

## 5. Conclusions

In this study, we established the efficient hepatocyte differentiation method which employs not only stage-specific transient overexpression of hepatocyte-related transcription factors but also 3D spheroid culture systems by using Nanopillar Plate. To the best of our knowledge, this is the first study in which the hepatocyte-like cells, having enough hepatocyte functions, mediate drug-induced cytotoxicity against many compounds. Our hepatocyte-like cells differentiated from hESCs or hiPSCs have potential to be applied in drug toxicity testing.

## Acknowledgments

We thank Misae Nishijima and Hiroko Matsumura for their excellent technical support. HM, KK, MKF, and TH were supported by grants from the Ministry of Health, Labor, and Welfare of Japan. HM was also supported by Japan Research foundation For Clinical Pharmacology, and The Uehara Memorial Foundation. MKF was also supported by Japan Society for the Promotion of Science Grant-in-Aid for Scientific Research. FS was supported by Program for Promotion of Fundamental Studies in Health Sciences of the National Institute of Biomedical Innovation (NIBIO). We thank Hiromu Yamada (NIBIO) for helpful discussion.

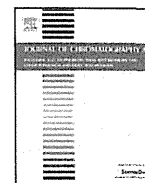
## Appendix A. Supplementary data

Supplementary data related to this article can be found at <http://dx.doi.org/10.1016/j.biomaterials.2012.11.029>.

## References

- [1] Thomson JA, Itskovitz-Eldor J, Shapiro SS, Waknitz MA, Swiergiel JJ, Marshall VS, et al. Embryonic stem cell lines derived from human blastocysts. *Science* 1998;282:1145–7.
- [2] Takahashi K, Tanabe K, Ohnuki M, Narita M, Ichisaka T, Tomoda K, et al. Induction of pluripotent stem cells from adult human fibroblasts by defined factors. *Cell* 2007;131:861–72.
- [3] Inamura M, Kawabata K, Takayama K, Tashiro K, Sakurai F, Katayama K, et al. Efficient generation of hepatoblasts from human ES cells and iPSC cells by transient overexpression of homeobox gene *HEX*. *Mol Ther* 2011;19:400–7.
- [4] Takayama K, Inamura M, Kawabata K, Tashiro K, Katayama K, Sakurai F, et al. Efficient and directive generation of two distinct endoderm lineages from human ESCs and iPSCs by differentiation stage-specific *SOX17* transduction. *PLoS One* 2011;6:e21780.
- [5] Takayama K, Inamura M, Kawabata K, Katayama K, Higuchi M, Tashiro K, et al. Efficient generation of functional hepatocytes from human embryonic stem cells and induced pluripotent stem cells by *HNF4alpha* transduction. *Mol Ther* 2012;20:127–37.
- [6] Takayama K, Inamura M, Kawabata K, Sugawara M, Kikuchi K, Higuchi M, et al. Generation of metabolically functioning hepatocytes from human pluripotent stem cells by *FOXA2* and *HNF1alpha* transduction. *J Hepatol* 2012;57:628–36.
- [7] Ramasamy TS, Yu JS, Selden C, Hodgson H, Cui W. Application of three-dimensional culture conditions to human embryonic stem cell-derived

- definitive endoderm cells enhances hepatocyte differentiation and functionality. *Tissue Eng Part A*. <http://dx.doi.org/10.1089/ten.tea.2012.0190>. Available from URL: <http://www.ncbi.nlm.nih.gov/pubmed/23003670>; 2012.
- [8] Nagamoto Y, Tashiro K, Takayama K, Ohashi K, Kawabata K, Sakurai F, et al. The promotion of hepatic maturation of human pluripotent stem cells in 3D co-culture using type I collagen and Swiss 3T3 cell sheets. *Biomaterials* 2012;33:4526–34.
- [9] Meng Q, Haque A, Hexig B, Alkaik T. The differentiation and isolation of mouse embryonic stem cells toward hepatocytes using galactose-carrying substrata. *Biomaterials* 2012;33:1414–27.
- [10] Shiraki N, Yamazoe T, Qin Z, Ohgomori K, Mochitate K, Kume K, et al. Efficient differentiation of embryonic stem cells into hepatic cells in vitro using a feeder-free basement membrane substratum. *PLoS One* 2011;6:e24228.
- [11] Takahashi R, Sonoda H, Tabata Y, Hisada A. Formation of hepatocyte spheroids with structural polarity and functional bile canaliculi using nanopillar sheets. *Tissue Eng Part A* 2010;16:1983–95.
- [12] Tong JZ, Sarrazin S, Cassio D, Gauthier F, Alvarez F. Application of spheroid culture to human hepatocytes and maintenance of their differentiation. *Biol Cell* 1994;81:77–81.
- [13] Bi YA, Kazolias D, Duignan DB. Use of cryopreserved human hepatocytes in sandwich culture to measure hepatobiliary transport. *Drug Metab Dispos* 2006;34:1658–65.
- [14] Makino H, Toyoda M, Matsumoto K, Saito H, Nishino K, Fukawatase Y, et al. Mesenchymal to embryonic incomplete transition of human cells by chimeric OCT4/3 (POU5F1) with physiological co-activator EWS. *Exp Cell Res* 2009;315:2727–40.
- [15] Nagata S, Toyoda M, Yamaguchi S, Hirano K, Makino H, Nishino K, et al. Efficient reprogramming of human and mouse primary extra-embryonic cells to pluripotent stem cells. *Genes Cells* 2009;14:1395–404.
- [16] Furue MK, Na J, Jackson JP, Okamoto T, Jones M, Baker D, et al. Heparin promotes the growth of human embryonic stem cells in a defined serum-free medium. *Proc Natl Acad Sci U S A* 2008;105:13409–14.
- [17] Kawabata K, Inamura M, Mizuguchi H. Efficient hepatic differentiation from human iPSC cells by gene transfer. *Methods Mol Biol* 2012;826:115–24.
- [18] Mizuguchi H, Kay MA. Efficient construction of a recombinant adenovirus vector by an improved in vitro ligation method. *Hum Gene Ther* 1998;9:2577–83.
- [19] Mizuguchi H, Kay MA. A simple method for constructing E1- and E1/E4-deleted recombinant adenoviral vectors. *Hum Gene Ther* 1999;10:2013–7.
- [20] Tashiro K, Kawabata K, Sakurai H, Kurachi S, Sakurai F, Yamanishi K, et al. Efficient adenovirus vector-mediated PPAR gamma gene transfer into mouse embryoid bodies promotes adipocyte differentiation. *J Gene Med* 2008;10:498–507.
- [21] Maizel Jr JV, White DO, Scharff MD. The polypeptides of adenovirus. I. Evidence for multiple protein components in the virion and a comparison of types 2, 7A, and 12. *Virology* 1968;36:115–25.
- [22] Yasumiba S, Tazuma S, Ochi H, Chayama K, Kajiyama G. Cyclosporin A reduces canalicular membrane fluidity and regulates transporter function in rats. *Biochem J* 2001;354:591–6.
- [23] Roman ID, Fernandez-Moreno MD, Fueyo JA, Roma MG, Coleman R. Cyclosporin A induced internalization of the bile salt export pump in isolated rat hepatocyte couplets. *Toxicol Sci* 2003;71:276–81.
- [24] Rodriguez-Antona C, Donato MT, Boobis A, Edwards RJ, Watts PS, Castell JV, et al. Cytochrome P450 expression in human hepatocytes and hepatoma cell lines: molecular mechanisms that determine lower expression in cultured cells. *Xenobiotica* 2002;32:505–20.
- [25] Hewitt NJ, Hewitt P. Phase I and II enzyme characterization of two sources of HepG2 cell lines. *Xenobiotica* 2004;34:243–56.
- [26] Gallagher EP, Kunze KL, Stapleton PL, Eaton DL. The kinetics of aflatoxin B1 oxidation by human cDNA-expressed and human liver microsomal cytochromes P450 1A2 and 3A4. *Toxicol Appl Pharmacol* 1996;141:595–606.
- [27] Lee MH, Graham GG, Williams KM, Day RO. A benefit-risk assessment of benzbromarone in the treatment of gout. Was its withdrawal from the market in the best interest of patients? *Drug Saf* 2008;31:643–65.
- [28] Glicklis R, Merchuk JC, Cohen S. Modeling mass transfer in hepatocyte spheroids via cell viability, spheroid size, and hepatocellular functions. *Biotechnol Bioeng* 2004;86:672–80.
- [29] Kim K, Ohashi K, Utoh R, Kano K, Okano T. Preserved liver-specific functions of hepatocytes in 3D co-culture with endothelial cell sheets. *Biomaterials* 2012;33:1406–13.
- [30] Khetani SR, Bhatia SN. Microscale culture of human liver cells for drug development. *Nat Biotechnol* 2008;26:120–6.
- [31] Iwamura A, Fukami T, Hosomi H, Nakajima M, Yokoi T. CYP2C9-mediated metabolic activation of losartan detected by a highly sensitive cell-based screening assay. *Drug Metab Dispos* 2011;39:838–46.
- [32] Hosomi H, Akai S, Minami K, Yoshikawa Y, Fukami T, Nakajima M, et al. An in vitro drug-induced hepatotoxicity screening system using CYP3A4-expressing and gamma-glutamylcysteine synthetase knockdown cells. *Toxicol In Vitro* 2010;24:1032–8.
- [33] Guengerich FP, MacDonald JS. Applying mechanisms of chemical toxicity to predict drug safety. *Chem Res Toxicol* 2007;20:344–69.
- [34] Hosomi H, Fukami T, Iwamura A, Nakajima M, Yokoi T. Development of a highly sensitive cytotoxicity assay system for CYP3A4-mediated metabolic activation. *Drug Metab Dispos* 2011;39:1388–95.



## Quality assurance of monoclonal antibody pharmaceuticals based on their charge variants using microchip isoelectric focusing method



Mitsuhiro Kinoshita<sup>a</sup>, Yuki Nakatsuji<sup>a</sup>, Shigeo Suzuki<sup>a</sup>,  
Takao Hayakawa<sup>b</sup>, Kazuaki Kakehi<sup>a,\*</sup>

<sup>a</sup> Faculty of Pharmacy, Kinki University, Kowakae 3-4-1, Higashi, Osaka 577-8502, Japan

<sup>b</sup> Pharmaceutical Research and Technology Institute, Kinki University, Kowakae 3-4-1, Higashi, Osaka 577-8502, Japan

### ARTICLE INFO

#### Article history:

Received 13 June 2013

Received in revised form 25 July 2013

Accepted 6 August 2013

Available online 13 August 2013

#### Keywords:

Antibody

Isoelectric focusing

Microchip

Charge variant

### ABSTRACT

Monoclonal antibody (mAb) pharmaceuticals are much more complex than small-molecule drugs. Such complex characteristics raise challenging questions for regulatory evaluation. Although heterogeneity in mAbs based on their charge variants has been mainly evaluated using gel-based isoelectric focusing (IEF) method, recent development in capillary electrophoresis and microchip electrophoresis has made it possible to assure their heterogeneities in more easy and rapid manner. In the present paper, we customized the imaged microchip isoelectric focusing (mIEF) for the analysis of mAbs, and compared the customized version with the conventional capillary isoelectric focusing (cIEF) method, and found that mIEF has much higher performance in operations, and its resolving powers are comparable with those obtained by cIEF.

© 2013 Elsevier B.V. All rights reserved.

### 1. Introduction

Clinical success of monoclonal antibody (mAb) pharmaceuticals has been transforming the pharmaceutical industries. In 2010, worldwide sales of all biologics including mAbs reached the US \$100 billion mark [1].

mAb is a large glycoprotein molecule, and has complex tertiary structure due to various post-translational modifications [2]. In addition, during manufacturing processes and storage periods of an mAb product, it is well known that modifications such as deamidation, C-terminal lysine variants, N-terminal pyroglutamate, glycation, and glycosylation are observed individually and/or simultaneously [3,4]. These modifications lead changes of charge heterogeneity in mAbs, and result in changes of the product characteristics, like long-term stability and binding activity. Thus detailed monitoring and controlling these modifications which can affect mAbs' characteristics are mandatory requirement by regulatory agencies [5].

For evaluation of charge heterogeneities in glycoproteins, slab gel isoelectric focusing (IEF) developed by Svensson in early 1960s [6] has been a major technique, and still widely being employed in the development of protein-based biopharmaceutical products for lot release, stability testing, formulation screening, process

development, comparability assessment, and product characterization. However, slab gel IEF method is time consuming and labor intensive. In addition, quantitative evaluation of the observed bands (spots) is not practical. Thus, most biopharmaceutical companies have shifted efforts into developing capillary based IEF assays. The capillary isoelectric focusing (cIEF) method was first introduced in 1985 by Hjerten and Zu using on-line direct UV detection [7]. The method involves a two-step process: the analytes are first focused in the capillary, and then the focused proteins are forced to move toward the on-line UV detector. This cIEF method is more robust, reproducible, and quantitative than slab gel IEF, and it has been successfully applied to many therapeutic glycoproteins including mAbs [5,8–10].

A different cIEF technique called imaged cIEF which employs the whole capillary imaging technology to detect the focused protein without the mobilization step was first demonstrated by Wu and Pawliszyn in 1992 [11,12]. The imaged capillary isoelectric focusing (icIEF) method is faster than the conventional on-line detection cIEF (typically, total run time is 20 min versus 60 min, respectively). Reproducibilities in the icIEF method are slightly better than cIEF, because icIEF method does not require mobilization step that causes disruption of pH gradient and diffusion of focused samples. The icIEF technology has been increasingly used in the field of biopharmaceuticals, and it is now becoming one of the tools to evaluate charge heterogeneity for the evaluation of many therapeutic glycoprotein products [13–15] and protein-based vaccines [16,17].

\* Corresponding author. Tel.: +81 6 4307 4001; fax: +81 6 6721 2353.  
E-mail address: [k.kakehi@phar.kindai.ac.jp](mailto:k.kakehi@phar.kindai.ac.jp) (K. Kakehi).

A quartz microchip-based apparatus with a linear imaging UV photodiode array detection (Shimadzu MCE-2010 system) was also commercially available and used in the IEF analysis of proteins. Vlcková et al. reported the results of IEF analysis of some biopharmaceuticals using the installed quartz microchip coated with linear polyacrylamide [18]. Three therapeutic proteins, hirudin, erythropoietin, and bevacizumab as a model of mAb were successfully analyzed, and the results were compared with conventional capillary IEF in terms of peak profile, isoelectric point ( $pI$ ) values, and reproducibility. Kitagawa et al. reported high-speed analysis of some proteins by a customized microchip IEF apparatus [19], which has a device for a simple straight channel chip. A standard mixture of some proteins was successfully separated into individual proteins having different  $pI$  values.

Based on these previous works, we customized the microchip apparatus for routine works in evaluation of charge variants of mAb products. An ultra-fast charge variant profiling which enables to evaluate biopharmaceutical glycoprotein products was estimated. The quartz chip having simple, short, and straight non-coated channel with whole column imaging detection system was investigated in terms of assay speed, throughput and the charge profiles, and the results were compared with those acquired by cIEF.

In addition, effects of the attached glycans and C-terminal lysine residues on charge variants of mAbs were also investigated. This is important information for evaluation of quality of mAb products.

## 2. Materials and methods

### 2.1. Reagents

All mAb products, bevacizumab, trastuzumab and cetuximab, were kindly donated by Kinki University Nara Hospital. Transferrin (human blood plasma) was purchased from Sigma–Aldrich (St. Louis, MO). Carrier ampholytes, ranges of pH 3–10, 5–8 and 8–10.5, were obtained from GE Healthcare (Buckinghamshire, UK). All  $pI$  markers ( $pI=5.12, 7.40, 8.18, 9.22, \text{ and } 10.10$ ) were from ProteinSimple (Santa Clara, CA). Iminodiacetic acid and hydroxypropyl methyl cellulose (HPMC; viscosity of 2% aqueous solution at 20 °C, 4000 cP) were purchased from Tokyo Kasei (Chu-o-ku, Tokyo, Japan) and Sigma–Aldrich, respectively. All other reagents, L-arginine, L-aspartic acid, sodium hydroxide, phosphoric acid,  $N,N,N',N'$ -tetramethylethylenediamine (TEMED) were from Wako Pure Chemical Industries (Dosho-machi, Osaka, Japan). Peptide- $N^4$ -(acetyl- $\beta$ -D-glucosaminyl) asparagine amidase (PNGase F, EC 3.5.1.52, recombinant) and carboxypeptidase B (EC 3.4.17.2) were from Roche Diagnostics (Mannheim, Germany). Sialidase (from *Arthrobacter ureafaciens*) was purchased from Nakalai Tesque (Nakagyo-ku, Kyoto, Japan).

### 2.2. mIEF instrument

On-chip measurements were performed on a commercial Shimadzu microchip electrophoresis system MCE-2010 (Kyoto, Japan), in which the chip design and the device for application of voltage are modified for charge profiling purpose. The  $D_2$ -lamp based instrument possesses a diode array detector with 1024 elements located along the separation channel, and it provides a linear imaging UV detection during electrophoresis [20]. A non-coated quartz microchip (Fig. 1a) having two 9  $\mu$ L reservoirs at the each end of a simple, short, and straight separation channel, was provided from Shimadzu. The chip does not have the injection device, because the whole analytical path is filled with the sample solution. Changing the chip design as shown in Fig. 1 shows the

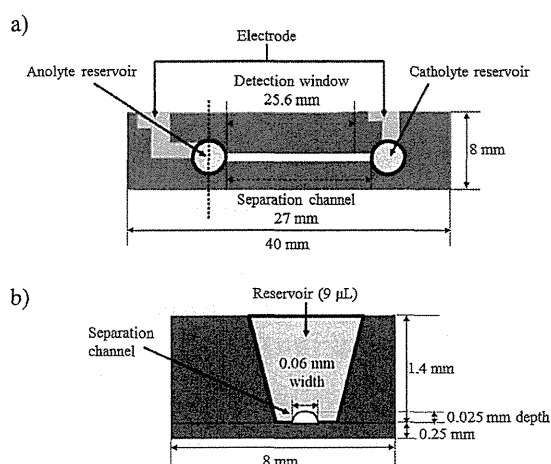


Fig. 1. (a) A quartz microchip specialized for isoelectric focusing, and (b) a scheme of a separation channel and a reservoir. Separated sample zones are monitored during electrophoresis within the detection window of 25.6 mm from the anolyte reservoir.

best ability in isoelectric focusing (IEF) analysis. The semielliptical channel fabricated onto a quartz-chip plate is 25- $\mu$ m depth and 60- $\mu$ m width as shown in Fig. 1b. The effective separation length and the imaging detection window are 27 mm and 25.6 mm, respectively. There are two platinum electrodes on the chip to apply voltages between the anolyte and catholyte reservoirs.

### 2.3. Preparation of the sample solution for IEF analyses

All mAb preparations were desalted by passing the solution through an ultrafiltration filter (Vivaspin 500; molecular weight cut-off: 100,000, GE Healthcare), and diluted with water to make aqueous 10 mg/mL solutions. The aqueous solution of transferrin (10 mg/mL) was also prepared in the same manner. The desalting procedure is especially important to obtain robust results in mIEF.

Sample solutions for mIEF analysis were prepared by mixing the protein solution with pharmalytes (pH 3–10, 5–8, and 8–10.5), HPMC solutions at different concentrations, suitable two  $pI$  markers (1  $\mu$ L each) that are observed at both acidic and basic ends of the mAb peaks, 200 mmol/L arginine and water. For cIEF analysis, 4  $\mu$ L of pharmalyte 3–10, 2  $\mu$ L of TEMED, 200  $\mu$ L of 0.8% (w/v) HPMC, 1  $\mu$ L of two  $pI$  markers and 8  $\mu$ L of 10 mg/mL antibody solution were mixed and diluted with water to make 400  $\mu$ L of sample solutions. Final concentrations of each component are: 1% (v/v) pharmalyte 3–10, 0.5% (v/v) TEMED, 0.4% (w/v) HPMC, and 0.2 mg/mL mAb.

### 2.4. Digestion of cetuximab with carboxypeptidase B and sialidase

For hydrolysis of C-terminal lysine residue on heavy chain, a solution of cetuximab (10 mg/mL, 100  $\mu$ L) was diluted with 20 mM phosphate buffer (pH 7.2, 100  $\mu$ L), and mixed with 2  $\mu$ L of carboxypeptidase B solution (1.5 U). The mixture was incubated at 37 °C for 12 h. After enzyme reaction, the reaction mixture was dialyzed against distilled water and lyophilized to dryness. The solution of carboxypeptidase-treated cetuximab (10 mg/mL, 100  $\mu$ L) was diluted with 20 mM sodium acetate buffer (pH 5.0, 100  $\mu$ L), and mixed with 2  $\mu$ L of sialidase solution (2 mU). The mixture was kept at 37 °C for 12 h, and dialyzed against distilled water, and lyophilized to dryness. The dried samples thus obtained were

**Table 1**  
Stepwise applied voltage for mIEF.

| Peptide marker |             | Transferrin |             | mAbs     |             |
|----------------|-------------|-------------|-------------|----------|-------------|
| Time (s)       | Voltage (V) | Time (s)    | Voltage (V) | Time (s) | Voltage (V) |
| 0–20           | 130         | 0–20        | 130         | 0–20     | 100         |
| 20–100         | 250         | 20–40       | 250         | 20–120   | 200         |
| 100–240        | 500         | 40–100      | 500         | 120–220  | 390         |
|                |             | 100–200     | 1000        | 220–270  | 780         |
|                |             |             |             | 270–380  | 1560        |

dissolved in distilled water to make 10 mg/mL concentration, and used for the analysis.

### 2.5. mIEF analysis

A bare silica chip was employed throughout all mIEF experiments. Prior to the mIEF measurement, both channel and reservoirs were rinsed with water 3 times from one end of the channel by applying suitable pressure using a syringe filled with water. Between measurements, the chip was rinsed with water 5 times. After removing water by applying air pressure with a syringe, the anolyte reservoir was filled with the sample solution and pressure was applied to the reservoir by a syringe in order to fill the channel with the sample solution. The anolyte and catholyte reservoirs were then emptied. And the anolyte reservoir was filled with anolyte (40 mmol/L of aspartic acid containing 1.0% (w/v) HPMC), and the catholyte reservoir was filled with catholyte (100 mmol/L of sodium hydroxide with 1.0% (w/v) HPMC). Focusing was performed by applying voltage as indicated in Table 1.

Microchip used in this study is specially modified and has a large reservoir volume (9  $\mu$ L) for catholyte and anolyte. Therefore, applying of constant high electric field strength (e.g. 450 V/cm) causes current burst at early stage of electrophoresis. Adopted stepwise voltage program could reduce initial current burst which causes migration of sample ions toward cathode with electroosmotic flow, and also could keep constant current during focusing. Detection was performed at 280 nm with monitoring the progress of the separation. The final image of the IEF trace was then converted to a data file for data analysis.

### 2.6. cIEF analysis

A P/ACE capillary electrophoresis system (Beckman Coulter, Fullerton, CA) equipped with a filter-based UV detector set at 280 nm was applied for cIEF measurements. Separations were carried out at 20 °C using a commercially available DB-1 capillary (internal diameter, 50  $\mu$ m, Agilent Technologies, Palo Alto, CA) with an effective length of 30 cm (total length, 40 cm). The capillary was rinsed with 6 mol/L urea for 10 min and then with water for 10 min prior to use. At the initial step, the capillary was filled with the sample solution by applying pressure (30 psi) for 2 min. During cIEF separation, 200 mmol/L of phosphoric acid containing 0.4% (w/v) HPMC was used as the anode buffer, and 300 mmol/L of sodium hydroxide containing 0.4% (w/v) HPMC was used as the cathode buffer. For focusing step, voltage at 25 kV in normal polarity was applied for 10 min to focus charge variants into their *pI* positions. For mobilization of the separated zones toward detection window, voltage at 25 kV in normal polarity was applied, and pressure at 0.5 psi was also added to both negative and positive ends of the capillary. The mobilized sample zones were detected at 280 nm. Between IEF analyses, the capillary was rinsed for 5 min with 6 mol/L urea, and then with water for 5 min. All the data were analyzed by 32 Karat software, version 8.0 (Beckman Coulter).

## 3. Results and discussion

### 3.1. Optimization studies for mIEF

At the initial step of optimization studies on mIEF analysis, transferrin (human, isoelectric point of the major isoform, ca. 5.4 [21]) was employed as model protein, because isoforms of transferrin have been extensively examined for clinical tests of chronic alcoholism [22–24]. Transferrin has two possible *N*-glycan attaching sites, and major *N*-glycans observed in transferrin are disialo-biantennary glycans, and trisialo-triantennary glycans are also present as minor glycans [25]. Four parameters (a) neutral polymer, (b) Pharmalyte, (c) mixing ratios of different *pI* range Pharmalyte, and (d) urea, were optimized (Table 2).

#### 3.1.1. Effect of neutral polymer concentration

Hydroxypropylmethylcellulose (HPMC, a commonly used neutral polymer) was used as an additive for mIEF to reduce electroosmotic flow during separation. Addition of a neutral polymer in the running buffer covers the silica surface and prevents the irreversible adsorption of the protein molecules to the quartz channel [26–28]. Therefore, the presence of the neutral polymer in the electrolyte improves the sensitivity as well as durability of the quartz chip. The sample solution for mIEF was prepared by mixing an aqueous solution (10 mg/mL: 20  $\mu$ L) of transferrin, 1  $\mu$ L of *pI* markers (*pI* 5.12 and 7.40), and HPMC solutions containing different concentrations of Pharmalyte 5–8. Isoforms of transferrin were not resolved well in a range of 0–0.1% of HPMC probably due to non-specific adsorption of the protein to the channel wall (Fig. 2a-1 and -2), because the peak intensities are smaller than those observed at higher concentrations of HPMC. When higher concentrations than 0.4% of HPMC were used (Fig. 2a-4 and -5), peaks became broader probably due to molecular sieving effect provided by HPMC [29,30]. Yasui et al. investigated the correlation between electrophoretic mobility of non-denatured proteins and HPMC concentration below 1.0% [31], which is much lower than the reported entanglement point [32]. HPMC has amphiphilic properties, and shows non-specific interactions with proteins at high concentrations [31] (Fig. 2a-4 and -5). From these reasons, 0.2% HPMC concentration (Fig. 2a-3) was selected.

#### 3.1.2. Pharmalyte concentration and its mixing ratios

In the present study, we chose Pharmalyte as carrier ampholyte due to the robustness in IEF analysis [5]. In order to achieve the best resolution among isoform peaks of transferrin, Pharmalyte concentration was investigated. At the lower concentrations than 1.0% of Pharmalyte, transferrin showed broad peak due to incomplete formation of pH gradient in the channel (Fig. 2b-1 and -2). On the other hand, broad peaks were also observed at the concentrations of 4.0% or 8.0% of Pharmalyte, although relatively sharp peaks of *pI* markers were observed (Fig. 2b-4 and -5). At 2.4% concentration of Pharmalyte, transferrin showed the similar electropherogram as reported previously [33] (Fig. 2b-3).

**Table 2**  
Parameters on optimization studies in mIEF.

| Parameter group | No. | HPMC concentration | Pharmalyte concentration | Mixing ratios of pharmalyte |      | Urea concentration (mol/L) |
|-----------------|-----|--------------------|--------------------------|-----------------------------|------|----------------------------|
|                 |     |                    |                          | 5–8                         | 3–10 |                            |
| (a)             | –1  | 0.0%               | 2.4%                     | 1                           | 0    | 0                          |
|                 | –2  | 0.1%               | 2.4%                     | 1                           | 0    | 0                          |
|                 | –3  | 0.2%               | 2.4%                     | 1                           | 0    | 0                          |
|                 | –4  | 0.4%               | 2.4%                     | 1                           | 0    | 0                          |
|                 | –5  | 0.8%               | 2.4%                     | 1                           | 0    | 0                          |
| (b)             | –1  | 0.2%               | 0.5%                     | 1                           | 0    | 0                          |
|                 | –2  | 0.2%               | 1.0%                     | 1                           | 0    | 0                          |
|                 | –3  | 0.2%               | 2.4%                     | 1                           | 0    | 0                          |
|                 | –4  | 0.2%               | 4.0%                     | 1                           | 0    | 0                          |
|                 | –5  | 0.2%               | 8.0%                     | 1                           | 0    | 0                          |
| (c)             | –1  | 0.2%               | 2.4%                     | 1                           | 0    | 0                          |
|                 | –2  | 0.2%               | 2.4%                     | 4                           | 1    | 0                          |
|                 | –3  | 0.2%               | 2.4%                     | 9                           | 1    | 0                          |
|                 | –4  | 0.2%               | 2.4%                     | 19                          | 1    | 0                          |
| (d)             | –1  | 0.2%               | 2.4%                     | 19                          | 1    | 0                          |
|                 | –2  | 0.2%               | 2.4%                     | 19                          | 1    | 1                          |
|                 | –3  | 0.2%               | 2.4%                     | 19                          | 1    | 2                          |

Mixing ratio of Pharmalyte products having different range of *pI*s to form the best pH gradient in the separation channel, is one of the key parameters to achieve the best resolution. Since transferrin possesses charge variants in a range of *pI* 5–7, several mixing ratios of Pharmalyte 3–10 and Pharmalyte 5–8 were examined. When Pharmalyte 3–10 and Pharmalyte 5–8 were used in 1:19 ratios (Fig. 2c–4), the best resolution of the peaks was observed as compared to the case using only Pharmalyte 5–8 (see Fig. 2b–3).

### 3.1.3. Addition of urea and TEMED

Urea is a commonly used additive for both cIEF and icIEF to increase solubility of hydrophobic proteins around their *pI* values [9,34], but urea denatures proteins, and often causes shifts of their *pI* values [11,35]. When urea was added to the separation mixture at 1 mol/L and 2 mol/L, *pI* values of the main peak were slightly shifted to the cathode and peak intensities were gradually decreased (Fig. 2d–2 and –3) probably due to denaturing of

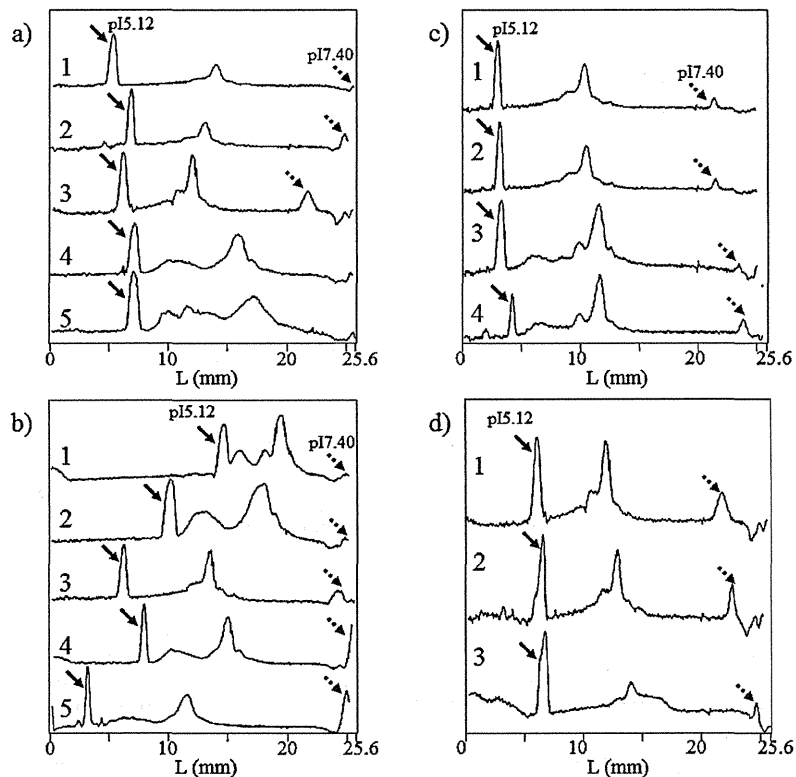


**Fig. 2.** mIEF separations at (a) several HPMC concentrations, (b) Pharmalyte concentrations, (c) Pharmalyte mixing ratios, and (d) urea concentrations in the separation mixture. Solid arrows and dashed arrows show *pI* markers of 5.12 and 7.40, respectively. (a) Sample solutions containing (1) 0%, (2) 0.1%, (3) 0.2%, (4) 0.4%, and (5) 0.8% HPMC as final concentration. (b) Sample solution containing (1) 0.5%, (2) 1.0%, (3) 2.4%, (4) 4.0%, and (5) 8.0% Pharmalyte as final concentration. (c) Sample solution containing Pharmalyte 3–10 and 5–8 at (1) 0:1, (2) 1:4, (3) 1:9, and (4) 1:19 ratios to make 2.4% Pharmalyte as final concentration. (d) Sample solution containing (1) 0 mol/L, (2) 1 mol/L, and (3) 2 mol/L urea as final concentrations. Analytical conditions: anolyte, 0.04 mol/L aspartic acid with 1% HPMC; catholyte, 0.1 mol/L sodium hydroxide with 1% HPMC; stepwise separation voltages were applied as shown in Table 1. Detection: UV absorption at 280 nm. Four parameters on optimization studies for mIEF are listed in Table 2.

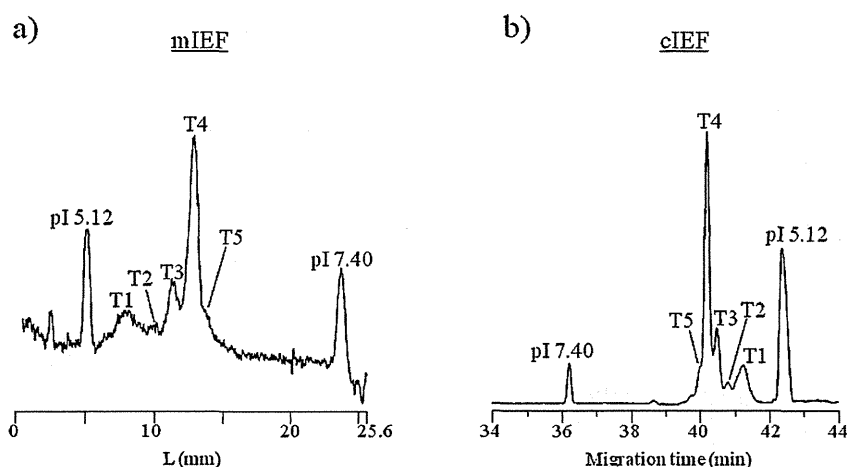


**Fig. 3.** mIEF (a) and cIEF (b) for profiling of charge variants of transferrin under optimized conditions. Peaks were labeled as T1 through T5 depending on their detection positions in mIEF. Smaller peak number means more acidic peak in the test sample. Analytical conditions for mIEF are the same as those in Fig. 2. Analytical conditions for cIEF: capillary, DB-1 capillary (Agilent Technologies), 50  $\mu$ m I.D. with an effective length of 30 cm (total length, 40 cm); anolyte, 0.2 mol/L phosphoric acid with 0.4% HPMC; catholyte, 0.3 mol/L sodium hydroxide with 0.4% HPMC; injection, 2 min at 30 psi; focusing, 25 kV in normal polarity for 10 min; mobilization, 25 kV in normal polarity with pressure at 0.5 psi on both negative and positive ends of capillary; temperature, 20 °C; detection, UV at 280 nm.

transferrin in the presence of urea at high concentrations [36]. In the analysis of transferrin, urea is not necessary (Fig. 2d-1).

TEMED is often used as an additive for preventing focusing of basic proteins beyond the detection window in cIEFs and works as a spacer between the catholyte and the basic end of pH gradient [35,37]. However, addition of TEMED in the separation mixture at 0.4% concentration obviously decreased resolution (data not shown). Thus, TEMED is not necessary in the analysis of isoforms of transferrin in mIEF. However, in case of the analysis of basic proteins having higher pI values (pI > 10), TEMED is required as a spacer.

Based on the optimization studies on the analysis of transferrin, the sample solution was prepared as follows: 2.4% of Pharmalyte (5–8:3–10, 19:1), 0.2% of HPMC and 2 mg/mL of transferrin.

#### 3.1.4. Analysis of isoforms of transferrin by mIEF and cIEF

Under the optimized conditions, transferrin was resolved into 5 isoforms within 200 s in a range of 5–15 mm from the anolyte reservoir (Fig. 3a). pI Values of the peaks were calculated by linear regression between pI 5.12 and 7.40 markers. Calculated pI value of the most abundant isoform (T4) was 6.06, and other isoforms (T1, T2, T3, and T5) were observed between pI 5.46 and 6.19 in mIEF analysis.

The calculated pI values obtained by mIEF were compared with those acquired by cIEF as shown in Fig. 3b. The difference ( $\Delta$ pI) of calculated pI values of the most abundant isoform (T4) was +0.14

(Table 3). And those of other isoforms (T1, T2, T3 and T5) ranged from –0.08 to +0.19. Thus, calculated pI values obtained by mIEF were comparable to those obtained by cIEF.

Sensitivities of the proposed mIEF system were slightly lower than those of cIEF system (see Fig. 3). The limit of detection (LOD) for transferrin (isoform T4) in mIEF was estimated to be ca. 0.2 mg/mL (as final concentration) from a signal to noise ratio (S/N = 3). On the other hand, LOD in cIEF was 0.005 mg/mL. Because the total length of the channel is 25 mm in mIEF, the amount of the injected sample is much smaller than cIEF. This is the major reason why high sensitivity is not achieved in mIEF. However, the proposed mIEF with linear imaging UV detection system does not need sample mobilization toward detection window which often causes diffusion of focused charge variants and disruption of pH gradient. Furthermore, we can monitor the progress of separations in the real-time manner, therefore, readily find the optimal conditions (see the movie for the analysis of transferrin in electronic supplementary materials).

#### 3.1.5. Effect of the presence of arginine in the sample solution

Most isoforms of mAb preparations show pI values between pI 7 and pI 10. Prior to the analysis of mAb, pH gradient formed during mIEF was examined using four pI markers (pIs 7.40, 8.18, 9.22, and 10.10) for accurate determination of pI values [5]. mIEF separation was performed using a mixture prepared by 2.4  $\mu$ L of pharmalyte 8–10.5, 34  $\mu$ L of 0.6% HPMC, 1  $\mu$ L of each pI marker,

**Table 3**  
Comparisons of calculated pI values in mIEF and cIEF.

| Peak number    | pI values in mIEF ( $\Delta$ pI) |              |              |              |
|----------------|----------------------------------|--------------|--------------|--------------|
|                | Transferrin                      | Bevacizumab  | Trastuzumab  | Cetuximab    |
| 1 (acidic end) | 5.46 (–0.08)                     | 7.96 (+0.09) | 8.45 (–0.07) | 7.57 (–0.12) |
| 2              | 5.70 ( $\pm$ 0.00)               | 8.10 (+0.07) | 8.57 (–0.05) | 7.71 (–0.16) |
| 3              | 5.88 (+0.06)                     | 8.29 (+0.05) | 8.76 (+0.02) | 7.90 (–0.14) |
| 4              | 6.06 (+0.14)                     | 8.41 (–0.01) | 8.89 (+0.04) | 8.09 (–0.15) |
| 5              | 6.19 (+0.19)                     | –            | 8.98 (+0.03) | 8.26 (–0.16) |
| 6              | –                                | –            | –            | 8.43 (–0.18) |
| 7              | –                                | –            | –            | 8.57 (–0.19) |
| 8 (basic end)  | –                                | –            | –            | 8.68 (–0.25) |

pI values obtained by mIEF are shown in the table. Numbers shown in round bracket are the actual pI difference ( $\Delta$ pI) compared with those obtained by conventional cIEF method. Peaks observed in each sample were labeled depending on their detection positions as shown in Figs. 3 and 5. Peak 1 means the most acidic-end peak in the sample, but they were not identical charge variants among the tested samples.

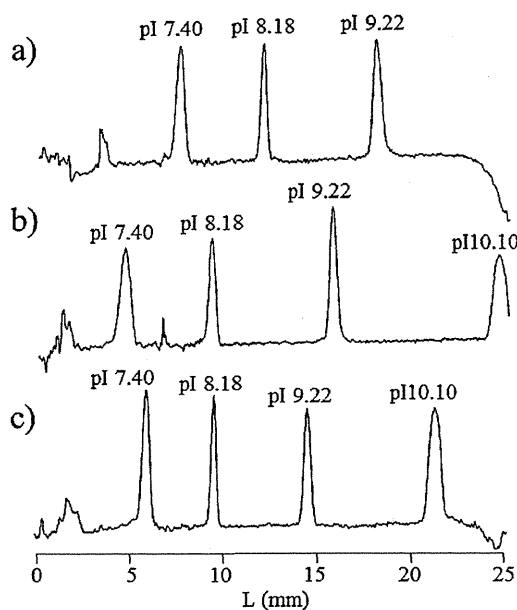


Fig. 4. MIEF separations of the mixture of four *pI* markers (*pI* 7.40, 8.18, 9.22, and 10.10) in the presence of (a) 0.0 mmol/L, (b) 4 mmol/L, and (c) 8 mmol/L arginine. Analytical conditions are the same as those in Fig. 2.

several volume of 200 mmol/L of arginine ( $pI = 10.76$ ) which is commonly used as cathodic stabilizer [9] and water to make the sample solution to 100  $\mu$ L. When analyzing the four *pI* markers without arginine, *pI* 10.10 marker was not detected due to leakage from the cathodic end (Fig. 4a). Addition of arginine to the mixture induced *pI* shift toward anodic end due to accumulated arginine zone at the cathodic end (Fig. 4b), and addition of 8 mmol/L of arginine showed the best separation of four *pI* markers within 240 s (Fig. 4c). Good linear relationship ( $R^2 = 0.983$ ) was observed between the *pI* values and distances of the *pI* markers from the anolyte reservoir.

### 3.2. MIEF analysis of mAb pharmaceuticals

The optimized conditions employed for the analysis of transferrin was applied to the analysis of commercially available mAb products (bevacizumab, trastuzumab, and cetuximab). The analytical conditions were slightly modified based on the *pI* values of each mAb preparation.

For MIEF of mAb products, the mixture containing 2.4% pharalyte 8–10.5, 0.2% HPMC, 8 mmol/L arginine and 2 mg/mL mAbs with two *pI* markers (*pI* 7.40 and 10.10) was employed as the sample solution. In bevacizumab, four charge variants (peak b1 to b4) were observed in both MIEF (Fig. 5a) and cIEF (Fig. 5b). *pI* values calculated by linear regression are summarized in Table 3.  $\Delta pI$  values were less than 0.09 for all observed peaks. And, relative abundances of the peaks (b1, b2, b3, and b4) were 4.0%, 23.5%, 69.2%, and 3.3% for MIEF, and were well correlated with the data observed by cIEF (5.0%, 24.9%, 64.8%, and 5.2%).

Other mAb products, trastuzumab (Fig. 5c) and cetuximab (Fig. 5e), were separated into five and eight charge variants by MIEF. Both electropherograms showed consistent profiles with those obtained by cIEF (Fig. 5d and f). The present data indicate that the proposed MIEF method is comparable to cIEF, and shows excellent ability in high-speed mAb analysis.

Table 4  
Intra- and inter-day assay variations of MIEF.

|                                    | Calculated <i>pI</i> values |      |      |      |
|------------------------------------|-----------------------------|------|------|------|
|                                    | b1                          | b2   | b3   | b4   |
| <i>Repeatability (intra-day)</i>   |                             |      |      |      |
| 1                                  | 7.86                        | 8.03 | 8.25 | 8.45 |
| 2                                  | 7.83                        | 8.00 | 8.22 | 8.42 |
| 3                                  | 7.86                        | 8.03 | 8.22 | 8.44 |
| Mean                               | 7.85                        | 8.02 | 8.23 | 8.44 |
| RSD (%)                            | 0.22                        | 0.22 | 0.21 | 0.21 |
| <i>Reproducibility (inter-day)</i> |                             |      |      |      |
| Day 1-1                            | 7.86                        | 8.02 | 8.22 | 8.43 |
| Day 1-2                            | 7.83                        | 8.00 | 8.21 | 8.40 |
| Day 1-3                            | 7.86                        | 8.04 | 8.22 | 8.43 |
| Day 2-1                            | 7.85                        | 8.05 | 8.25 | 8.46 |
| Day 2-2                            | 7.86                        | 8.05 | 8.23 | 8.46 |
| Day 2-3                            | 7.84                        | 8.02 | 8.25 | 8.44 |
| Day 3-1                            | 7.86                        | 8.03 | 8.25 | 8.45 |
| Day 3-2                            | 7.83                        | 8.00 | 8.22 | 8.42 |
| Day 3-3                            | 7.86                        | 8.03 | 8.22 | 8.45 |
| Mean                               | 7.85                        | 8.03 | 8.23 | 8.44 |
| RSD (%)                            | 0.17                        | 0.23 | 0.19 | 0.24 |

Peaks observed in bevacizumab were labeled as b1 through b4 depending on their detection positions as shown in Fig. 5a.

### 3.3. Precision of MIEF method

In order to evaluate the precision of the optimized MIEF method, repeatability and reproducibility were investigated using bevacizumab as a model mAb product. For repeatability assessment, a single separation mixture was prepared and analyzed using two *pI* markers of 7.40 and 9.22 instead of 10.10. On the other hand, for reproducibility assessment, separation mixtures were prepared in triplicate on each day, and analyzed by MIEF over three days as summarized in Table 4.

All four charge variants were separated each other within 380 s, and RSDs of the measured position (*L*, mm) ranged from 0.81% to 1.28% under optimized conditions (data not shown). After correction using *pI* markers, RSDs of calculated *pI* values were less than 0.25%. These values were comparable with those obtained by cIEF (0.2% or less in [15,38]). These data indicate that the proposed MIEF method shows excellent reproducibility, because the method does not require mobilization, and superior to those obtained by the conventional two-step cIEF [5]. In addition, RSDs of relative abundances of each peak (b1 to b4) in repeatability experiments (intra-day,  $n = 3$ ) were 9.5%, 0.7%, 1.7%, and 11.5%, and in reproducibility executions (inter-day,  $n = 9$ ) were 14.0%, 8.8%, 3.8%, and 16.6%, respectively. These values were similar to those reported previously using cIEF as described above.

### 3.4. Assessment of heterogeneity by sequential enzymatic digestions of mAb pharmaceuticals

C-Terminal lysine variants [39] and the presence of sialo *N*-glycans in mAb products [40] are the major reasons for charge variants. Two enzymes, carboxypeptidase B and sialidase, were used to understand charge heterogeneity of cetuximab. Digestion of cetuximab with carboxypeptidase B caused disappearance of two peaks (c7 and c8) at basic region (Fig. 6b).

In contrast, trastuzumab and bevacizumab (humanized antibody products manufactured by CHO cells) showed no significant changes (data not shown). These results are consistent with the previous report that relative amounts of incorporated C-terminal lysine in mAbs manufactured by CHO cell lines were up to 5% [40]. In addition, further digestion with sialidase resulted in



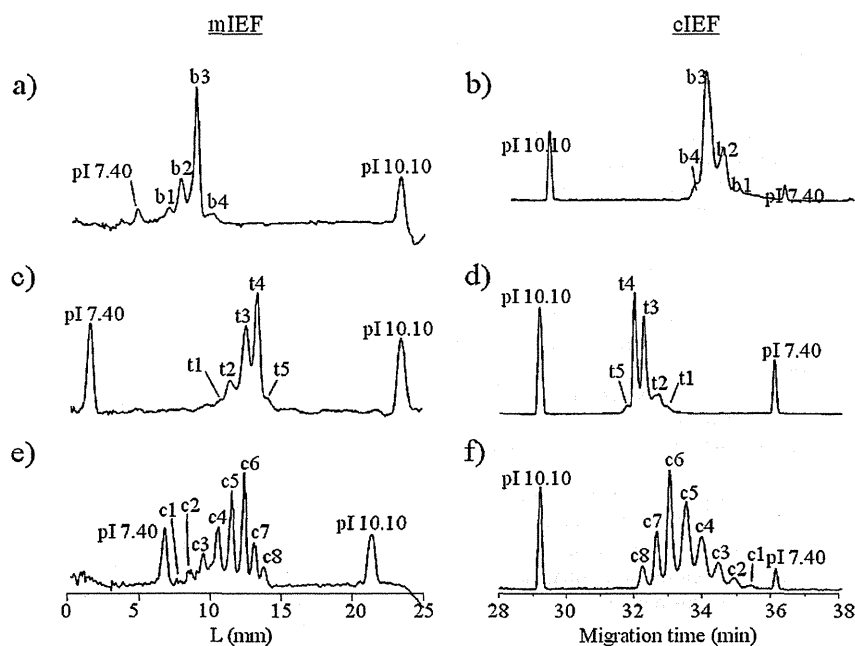


**Fig. 5.** Analysis of charge variants of bevacizumab, trastuzumab, and cetuximab by mIEF (left column) and cIEF (right column). Peaks observed in each sample were labeled with numbers depending on their detection positions. Peak 1 means the most acidic-end peak in the sample, but they were not identical charge variants among the tested samples. Analytical conditions are the same as shown in Fig. 2. Bevacizumab (a and b), trastuzumab (c and d) and cetuximab (e and f).

decrease/disappearance of the peaks observed in acidic pI regions (Fig. 6c). After successive digestion with these two enzymes, cetuximab gave the simple profile which is similar to that of bevacizumab and trastuzumab as shown in Fig. 5a and c. Thus, charge heterogeneity of cetuximab is largely due to C-terminal lysine processing and sialylation of *N*-glycans. These charge heterogeneities of cetuximab may be due to manufacturing process. Bevacizumab and trastumab are humanized mAb products (IgG<sub>1</sub>), and produced by

CHO cells. In contrast, cetuximab is chimeric mouse-human IgG<sub>1</sub> produced by mouse myeloma SP2/0 cell line. This means that manufacturing process change in cell type may lead significant alteration in mAb heterogeneity especially in charge variants. Several charge variants are still present in enzyme-treated cetuximab. Although cetuximab may include other possible modifications such as N-terminal glutamine cyclization, asparagine deamination, and methionine oxidation, detailed structural analysis will be necessary to get better understanding in heterogeneity of mAbs by analyzing fractionated peaks such as accurate mass spectrometric methods.

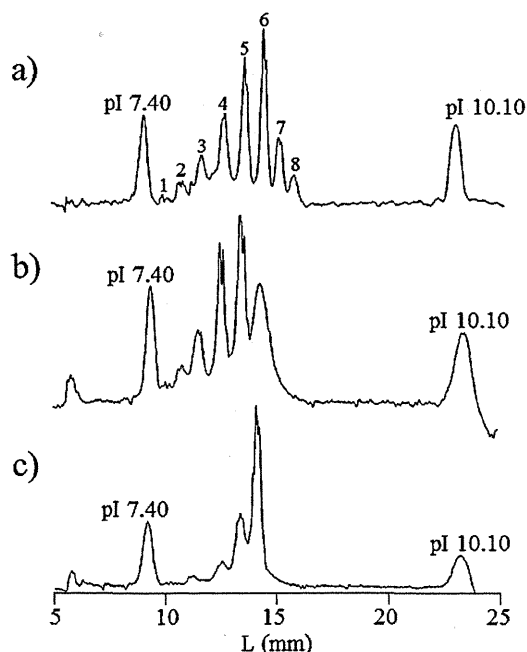


**Fig. 6.** mIEF separation of (a) intact, (b) carboxypeptidase B-treated, and (c) sialidase-treated cetuximab. Analytical conditions are the same as shown in Fig. 2.

#### 4. Conclusion

A combination of a quartz chip specialized for isoelectric focusing and a microchip electrophoresis system with a whole column imaging UV photodiode array detector achieved ultrafast evaluation of charge variants of glycoproteins. The quartz chip having a simple, short and straight channel without any coating could resolve transferrin and three mAb pharmaceuticals into their charge variants within 200 s and 380 s with high reproducibility in terms of calculated pI values and percent relative amounts of each charge variant.

Charge profiles of protein samples determined by mIEF well corresponded to those obtained by cIEF. When comparing precision in pI determination in mIEF measurements with icIEF measurements (e.g. commercially available iCE280 Analyzer), and cIEF, reproducibility of the calculated pI values is comparable to the iCE280 and superior to cIEF [15,38]. It should be noted that the time required for the analysis is much shorter than cIEF (approximately 10 times), which requires mobilization step after completion of focusing, and faster than icIEF (about 3 times) due to incorporation of shorter separation channel. Whole column imaging UV photodiode array detector leads precise tuning of focusing time, because the progress of the focusing can be monitored on the real-time basis. However, the proposed system needs to wash the chip manually, and further improvements in functionalization and

automation will be required for commercial use in the pharmaceutical industries. It is difficult to introduce enough amount of the sample due to short analytical channel. Improvement of the sensitivity is another future requirement.

Evaluation of charge heterogeneity is necessary for assurance of quality and stability of mAb products. Some charge variants derived from several post-translational modifications or degradation show different biological activity and stability compared to their original variants [41,42]. Isoelectric focusing based techniques such as mIEF, icIEF and cIEF makes us easy to access to useful information on product specific “fingerprint” derived from charge heterogeneity of biopharmaceuticals. To get much better understanding in detail into the therapeutics, further investigation such as structural analyses, potency, toxicity and stability evaluation will be required. Mass spectrometry is one of the powerful tools to satisfy these demands from the pharmaceutical industry, and fractionated/separated peaks need to be analyzed for further evaluation of their characterization.

The proposed ultrafast and precise mIEF method is easily applied to identity and purity analyses in product lot release, stability testing, formulation screening, process development, comparability assessment and product characterization of biopharmaceutical products possessing complex charge heterogeneity.

#### Acknowledgements

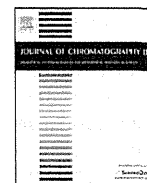
The authors would like to thank Dr. Eiki Maeda at Analytical Development Laboratories, CMC Center, Takeda Pharmaceutical Company Limited for experimental supports. The authors are also grateful to Shin Nakamura and Akihiro Arai at Life Science Business Department, Analytical & Measuring Instruments Division, Shimadzu Cooperation for providing microchip and measuring equipment.

#### Appendix A. Supplementary data

Supplementary data associated with this article can be found, in the online version, at <http://dx.doi.org/10.1016/j.chroma.2013.08.021>.

#### References

- [1] S.A. Berkowitz, J.R. Engen, J.R. Mazzeo, G.B. Jones, *Nat. Rev. Drug Discov.* 11 (2012) 527.
- [2] M. Mann, O.N. Jensen, *Nat. Biotechnol.* 21 (2003) 255.
- [3] O.N. Jensen, *Curr. Opin. Chem. Biol.* 8 (2004) 33.
- [4] J. Seo, K.-J. Lee, *J. Biochem. Mol. Biol.* 37 (2004) 35.
- [5] E. Maeda, K. Urakami, K. Shimura, M. Kinoshita, K. Kakehi, *J. Chromatogr. A* 1217 (2010) 7164.
- [6] H. Svensson, *Acta Chem. Scand.* 15 (1961) 325.
- [7] S. Hjertén, M.-d. Zhu, *J. Chromatogr.* 346 (1985) 265.
- [8] Y. Kuroda, H. Yukinaga, M. Kitano, T. Noguchi, M. Nemati, A. Shibukawa, T. Nakagawa, K. Matsuzaki, *J. Pharm. Biomed. Anal.* 37 (2005) 423.
- [9] J. Lin, Q. Tan, S. Wang, *J. Sep. Sci.* 34 (2011) 1696.
- [10] K.G. Moorhouse, C.A. Rickel, A.B. Chen, *Electrophoresis* 17 (1996) 423.
- [11] J. Wu, J. Pawliszyn, *Anal. Chem.* 64 (1992) 2934.
- [12] J. Wu, J. Pawliszyn, *Anal. Chem.* 64 (1992) 224.
- [13] P. Dou, Z. Liu, J. He, J.-J. Xu, H.-Y. Chen, *J. Chromatogr. A* 1190 (2008) 372.
- [14] X.Z. He, A.H. Que, J.J. Mo, *Electrophoresis* 30 (2009) 714.
- [15] Z. Sosic, D. Houde, A. Blum, T. Carlage, Y. Lyubarskaya, *Electrophoresis* 29 (2008) 4368.
- [16] L. Goodridge, C. Goodridge, J. Wu, M. Griffiths, J. Pawliszyn, *Anal. Chem.* 76 (2004) 48.
- [17] Z. Liu, J. Pawliszyn, *Electrophoresis* 26 (2005) 556.
- [18] M. Vlcková, F. Kalman, M.A. Schwarz, *J. Chromatogr. A* 1181 (2008) 145.
- [19] F. Kitagawa, S. Aizawa, K. Otsuka, *Anal. Sci.* 25 (2009) 979.
- [20] H. Nakanishi, T. Nishimoto, A. Arai, H. Abe, M. Kanai, Y. Fujiyama, T. Yoshida, *Electrophoresis* 22 (2001) 230.
- [21] H. Stibler, *Clin. Chem.* 37 (1991) 2029.
- [22] F. Crivellente, G. Fracasso, R. Valentini, G. Manetto, A.P. Riviera, F. Tagliaro, *J. Chromatogr. B: Biomed. Sci. Appl.* 739 (2000) 81.
- [23] F. Tagliaro, F. Bortolotti, M. Zuliani, F. Crivellente, G. Manetti, V.L. Pascoli, M. Marigo, *J. Capill. Electrophor. Microchip Technol.* 6 (1999) 137.
- [24] F. Tagliaro, F. Crivellente, G. Manetto, I. Puppi, Z. Deyl, M. Marigo, *Electrophoresis* 19 (1998) 3033.
- [25] E. Landberg, E. Aström, B. Kägedal, P. Pålsson, *Clin. Chim. Acta: Int. J. Clin. Chem.* 414C (2012) 58.
- [26] S.R. Bean, G.L. Lookhart, *Electrophoresis* 19 (1998) 3190.
- [27] P.G. Righetti, C. Gelfi, B. Verzola, L. Castelletti, *Electrophoresis* 22 (2001) 603.
- [28] M. Viehues, S. Manchanda, T.-C. Chao, D. Anselmetti, J. Regtmeier, *A. Ros. Anal. Bioanal. Chem.* 401 (2011) 2113.
- [29] B. Deng, N. Ye, G. Luo, Y. Wang, *J. Nanosci. Nanotechnol.* 5 (2005) 1193.
- [30] M.-Y. Ye, X.-F. Yin, Z.-L. Fang, *Anal. Bioanal. Chem.* 381 (2005) 820.
- [31] T. Yasui, M. Reza Mohamadi, N. Kaji, Y. Okamoto, M. Tokeshi, Y. Baba, *Biomed. Microfluidics* 5 (2011) 441141.
- [32] A.E. Barron, D.S. Soane, H.W. Blanch, *J. Chromatogr. A* 652 (1993) 3.
- [33] E. Quintana, R. Montero, M. Casado, A. Navarro-Sastre, M.A. Vilaseca, P. Briones, R. Artuch, *J. Chromatogr. B: Anal. Technol. Biomed. Life Sci.* 877 (2009) 2513.
- [34] S. Mack, I. Cruzado-Park, J. Chapman, C. Ratnayake, G. Vigh, *Electrophoresis* 30 (2009) 4049.
- [35] A. Cifuentes, M.V. Moreno-Arribas, M. de Frutos, J.C. Díez-Masa, *J. Chromatogr. A* 830 (1999) 453.
- [36] A. Pantazaki, M. Taverna, C. Vidal-Madjar, *Anal. Chim. Acta* 383 (1999) 137.
- [37] A. Bossi, P.G. Righetti, C. Visco, U. Breme, M. Mauriello, B. Valsasina, G. Orsini, E. Wenisch, *Electrophoresis* 17 (1996) 932.
- [38] N. Li, K. Kessler, L. Bass, D. Zeng, *J. Pharm. Biomed. Anal.* 43 (2007) 963.
- [39] L.W. Dick, D. Qiu, D. Mahon, M. Adamo, K.-C. Cheng, *Biotechnol. Bioeng.* 100 (2008) 1132.
- [40] E. Maeda, S. Kita, M. Kinoshita, K. Urakami, T. Hayakawa, K. Kakehi, *Anal. Chem.* 84 (2012) 2373.
- [41] G. Janini, N. Sapharishi, M. Waselus, G. Soman, *Electrophoresis* 23 (2002) 1605.
- [42] P.A. Trail, H.D. King, G.M. Dubowchik, *Cancer Immunol. Immunother.* 52 (2003) 328.



## Free glycans derived from glycoproteins present in human sera



Kinya Iwatsuka<sup>a</sup>, Sakie Watanabe<sup>a</sup>, Mitsuhiro Kinoshita<sup>a</sup>, Kazuya Kamisue<sup>a</sup>,  
Keita Yamada<sup>a</sup>, Takao Hayakawa<sup>b</sup>, Tadashi Suzuki<sup>c</sup>, Kazuaki Kakehi<sup>a,\*</sup>

<sup>a</sup> Faculty of Pharmaceutical Sciences, Kinki University, 3-4-1 Kowakae, Higashi-Osaka 577-8502, Japan

<sup>b</sup> Pharmaceutical Research and Technology Institute, Kinki University, Kowakae 3-4-1, Higashi-osaka 577-8502, Japan

<sup>c</sup> Glycometabolome Laboratory, Frontier Research System, RIKEN (The Institute for Physical and Chemical Research), 2-1 Hirosawa, Wako, Saitama 351-0198, Japan

### ARTICLE INFO

#### Article history:

Received 15 December 2012

Accepted 12 March 2013

Available online 21 March 2013

#### Keywords:

Free glycans

Serum

Transferrin

HPLC

ESI-TOF-MS

### ABSTRACT

During the course of studies on the analysis of O-glycans in biological samples, we found that significant amount of free glycans are present in normal human serum samples. The most abundant free glycan was disialo-biantennary glycan typically observed in transferrin which is one of the abundant glycoproteins found in sera. Minor glycans were also considered to be mainly due to transferrin, but some glycans were derived from mucin-type O-glycans, although the amount was quite minute. However, high mannose-type glycans could not be detected at all. Although there have been many reports on the presence of intracellular “free” N-glycans (mainly derived from high mannose-type glycans) generated either from lipid-linked oligosaccharides or from misfolded glycoproteins through endoplasmic-reticulum associated protein degradation pathway, there is little information on the presence of free glycans in extracellular matrix and biological fluids such as serum. This report is the first one which demonstrates the presence of free glycans due to glycoproteins in sera.

© 2013 Elsevier B.V. All rights reserved.

### 1. Introduction

There have been many reports on the presence of free glycans in cytosols, and the formation of such free glycans is an important clue for the understanding the selection of properly synthesized glycoproteins. Such free glycans found in cytosols are exclusively high mannose-type glycans having one N-acetylglucosamine (GlcNAc) residue at the reducing termini [1,2], and are formed in the cytosol by a cellular system called ERAD (endoplasmic reticulum-associated degradation) [3]. Such intracellular “free” N-glycans are generated either from lipid-linked oligosaccharides or from misfolded glycoproteins [4–7]. In both cases, occurrence of high mannose-type free glycans, which have one GlcNAc residue at their reducing ends, has been well-documented.

Little is known with regard to the accumulation of more processed, complex-type free glycans in the cytosol of mammalian cells. In our previous report on the comprehensive analysis of N-glycans in cancer cells [8], we found that significantly large amount of unusual, complex-type free N-glycans were accumulated in stomach cancer-derived cell lines, MKN7 and MKN45. It should be noticed that all the free glycans found in these cells were cleaved between the GlcNAc $\beta$ 1–4GlcNAc (i.e. chitobiose) bond and a single

GlcNAc residue was present at the reducing end. In addition, most of the accumulated glycans have N-acetylneuraminic acid (NeuAc) residues at the non-reducing termini. And we showed that loss of the activity of cytosolic neuraminidase, Neu2, was responsible for the accumulation of such unusual free glycans [9].

In contrast, there is little information on the presence of free glycans in extracellular matrixes and biological fluids such as sera probably due to insufficient and poor ability to analyze minute amount of glycans. We have been developing sensitive methods for comprehensive analyses of N- and O-glycans in biological samples, especially cancer cells, tissues and serum samples [5,10–13]. During the course of studies on the analysis of O-glycans in biological samples, we found that significant amount of free glycans are present in human serum samples. This is unexpected and interesting, although it is well known that patients suffering from genetic lysosomal disorders of complex carbohydrate metabolism excrete a considerable amount of unusual oligosaccharides in urine [14–17].

Inoue et al. reported that free glycans were present in the unfertilized eggs of a fresh water trout, *Plecoglossus altivelis* [18]. The isolated glycans consist of desialylated biantennary glycans with  $\beta$ -Man-GlcNAc structure at their reducing termini. However, a small portion of the glycans having chitobiose (GlcNAc $\beta$ 1–4-GlcNAc) structure at the reducing ends were also present. It is still not clear why and how such large amount of free glycans are accumulated in unfertilized eggs. Another important report on the presence of free glycans is the expression of free glycans in human seminal

\* Corresponding author. Tel.: +80 6 6721 2332; fax: +80 6 6721 2353.  
E-mail address: [k.kakehi@phar.kindai.ac.jp](mailto:k.kakehi@phar.kindai.ac.jp) (K. Kakehi).

plasma [19], and the structural characteristics are similar to those in human milk. But their variations are simpler than those of human milk oligosaccharides.

According to the reference search works on the presence of free glycans in sera, the present work demonstrating the presence of free glycans in sera is the first one, and will lead to a new research project on finding glycan-based disease biomarkers.

## 2. Materials and methods

### 2.1. Materials

Sephadex LH-20 and Asahi Shodex NH2P-50 4E column were obtained from GE Healthcare UK Ltd. (Buckinghamshire, UK) and Showa Denko (Minato-ku, Tokyo, Japan), respectively. Sodium cyanoborohydride and 2-aminobenzoic acid (2AA) were from Tokyo Kasei Kogyo (Chuo-Ku, Tokyo, Japan). TOYOPAK ODS-S for solid phase extraction was from Tosoh (Minato-ku, Tokyo, Japan). VIVASPIN 500 (3000 molecular weight cut off) for ultrafiltration was from Sigma–Aldrich Japan (Shinagawa-ku, Tokyo, Japan). All other reagents were of the highest grade commercially available. All aqueous solutions were prepared using water purified with a Milli-Q purification system (Millipore, Bedford, MA, USA).

### 2.2. Serum samples

Serum samples from healthy volunteers were obtained under the permission of the Ethics Committee of Kinki University School of Pharmacy, and used in accordance with the tenets of the Declaration of Helsinki.

### 2.3. Sample preparation

#### 2.3.1. Ultrafiltration and solid-phase extraction of the serum sample

Because the serum sample contains a large amount of low-molecular-weight materials such as monosaccharides (typically glucose) and inorganic salts, and hydrophobic compounds, these materials should be removed prior to the analysis.

A serum sample (25  $\mu$ L) was centrifuged at 15,000  $\times$  g using an ultramembrane filter (3000 molecular weight cut off) to remove the low-molecular weight materials, and concentrated to the one fourth volume. Water (150  $\mu$ L) was added to the concentrate on the membrane, and centrifuged at 15,000  $\times$  g again. The procedures were repeated three times. The concentrated serum sample on the membrane was transferred to a new tube, and the membrane was washed with water (150  $\mu$ L) and combined with the concentrated solution. The mixture was then passed through an ODS cartridge (90 mg) which was previously washed with methanol (0.8 mL  $3\times$ ) and water (0.8 mL  $3\times$ ). The clean-up procedures were performed according to the method recommended by the manufacturer.

#### 2.3.2. Total N-glycans in a serum sample

A serum sample (150  $\mu$ L) was centrifuged at 15,000  $\times$  g using an ultramembrane filter (3000 molecular weight cut off) to remove the low-molecular weight materials, and concentrated to dryness. The dried sample was suspended in water (200  $\mu$ L) and was mixed with 10% SDS (24  $\mu$ L) and 2-mercaptoethanol (2.4  $\mu$ L). The mixture was kept in the boiling water bath for 5 min. After cooling, 10% NP40 (nonylphenol poly(ethylene glycol ether)<sub>n</sub>) solution (24  $\mu$ L) and 1 M sodium phosphate buffer (pH 7.5, 29  $\mu$ L) were added. After addition of N-glycoamidase F (2 units), the mixture was kept at 37 °C overnight. After cooling, ethanol (695  $\mu$ L) was added and the mixture was centrifuged at 15,000  $\times$  g for 10 min. The supernatant was collected and evaporated to dryness under reduced pressure.

#### 2.3.3. Releasing reaction of O-glycans in mucin-type glycoproteins in serum samples

Releasing reaction of O-glycans from mucin-type glycoproteins present in serum samples was performed using the automated glycan releasing system according to the method reported previously [10].

#### 2.3.4. Fluorescent labeling of glycans with 2AA

The sample of glycan mixture was dissolved in water (20  $\mu$ L) and 2AA solution (100  $\mu$ L) which was freshly prepared by dissolution of 2AA (15 mg) and sodium cyanoborohydride (15 mg) in methanol (500  $\mu$ L) containing 4% sodium acetate and 2% boric acid. The mixture was kept at 80 °C for 1 h, and water (20  $\mu$ L) and 50% (v/v) methanol (200  $\mu$ L) were added to the mixture after cooling, and centrifuged at 15,000  $\times$  g for 10 min. The supernatant solution was applied to a column of Sephadex LH-20 (1.0 cm i.d., 30 cm length), which was previously equilibrated with 50% methanol. The earlier eluted fluorescent fractions were pooled and evaporated to dryness under reduced pressure. The residue was further purified by solid phase extraction as described above (Section 2.3.1), and evaporated to dryness.

#### 2.3.5. Digestion of the glycan mixture with neuraminidase

Neuraminidase (1 unit, 2  $\mu$ L) was added to the mixture of 2AA-labeled glycans in 20 mM acetate buffer (pH 5.0, 20  $\mu$ L), and the mixture was incubated at 37 °C overnight. After keeping the mixture in the boiling water bath for 10 min followed by centrifugation, the supernatant solution was used for MS analysis.

### 2.4. HPLC analysis of 2AA-labeled free glycans and N-glycans in serum samples

Analysis of the 2AA-labeled glycans was performed with two Shimadzu LC-10ADvp pumps, a Jasco FP-920 fluorescence detector equipped with a polymer-based Asahi Shodex NH2P-50 4E column (4.6 mm i.d.  $\times$  250 mm). Linear gradient method was employed by 2% acetic acid in acetonitrile (solvent A) and 5% acetic acid in water containing 3% triethylamine (solvent B). The column was initially equilibrated and eluted with 30% solvent B for 2 min. Then, solvent B was increased to 95% over 80 min, and kept at this composition for further 20 min. The column effluent was monitored by a fluorescence detector set at an excitation wavelength of 350 nm and 425 nm for emission.

### 2.5. Liquid chromatography–electrospray ionization ion-trap time-of-flight mass spectrometry (LC–ESI–IT–TOF MS)

Negative electrospray ionization (ESI)-MS analyses were conducted with an LC–IT–TOF MS instrument (Shimadzu) connected with an HPLC system (LC-20AD pump and CBM-20A system controller; Shimadzu). The 2AA-labeled glycans were analyzed by infusion method. Isocratic elution was carried out at a flow rate of 0.2 mL/min with 50% (v/v) acetonitrile in water. The MS apparatus was operated at a probe voltage of 1.75 kV, CDL temperature of 180 °C, nebulizer gas flow of 1.5 L/min, ion accumulation time of 30 ms. MS range was from *m/z* 200 to 2000. CID parameters were as follows: energy, 50%; collision gas, 50%. MS data were processed with LCMS solution ver. 3.6 software (Shimadzu).

## 3. Results and discussion

### 3.1. Free glycans in serum samples

Fig. 1a shows the results on the analysis of O-glycans in a serum sample. In this analysis, O-glycans were previously

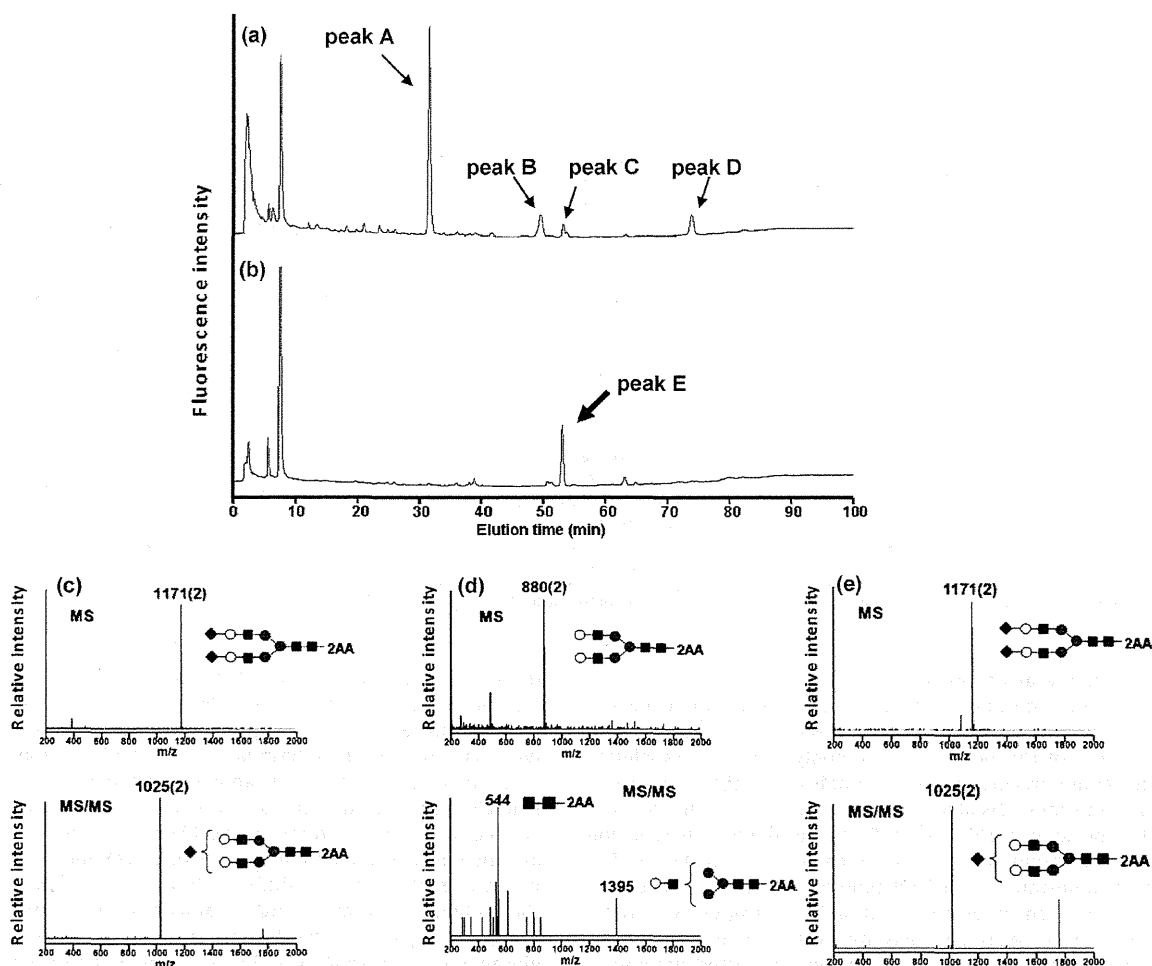


**Fig. 1.** HPLC Analysis of (a) mucin-type glycans from human serum released from the glycoproteins. (b) Intact serum sample after easy removal of low molecular weight materials. MS and MS/MS data of (c) peak C and (d) the product after neuraminidase digestion of peak C. (e) MS and MS/MS data of peak E. HPLC conditions: column, Asahi Shodex NH2P-50 4E(4.6 mm  $\times$  250 mm). Eluent solvent A, 2% acetic acid in acetonitrile, solvent B, 5% acetic acid, 3% triethylamine in water. Gradient condition: a linear gradient (30–95% solvent B) from 2 to 82 min, maintained for 20 min. Symbols: squares, N-acetylglucosamine; gray circles, mannose; white circles, galactose; diamonds, N-acetylneuraminic acid.

chemically released from the glycoproteins in a serum sample by an automatic manner developed by the authors [10–13], and analyzed by HPLC after labeling with a fluorescent reagent, 2AA. Four peaks (A–D) were detected at 30 (A), 46 (B), 53 (C) and 70 min (D), respectively. Peaks A, B and D were due to mucin-type O-glycans, and identified as sialyl T (NeuAc $\alpha$ 2-3Gal $\beta$ 1-3GalNAc-2AA), degradation product (NeuAc $\alpha$ 2-3 Gal) and disialyl T (NeuAc $\alpha$ 2-3Gal $\beta$ 1-3[NeuAc $\alpha$ 2-6]GalNAc-2AA), respectively. A distinct peak (peak C) other than those of mucin-derived glycans was observed at 53 min. The MS and MS/MS spectra of the peak C are shown in Fig. 1c. The molecular ion of the peak was observed at  $m/z$  1171 as a doubly charged ion, which was confirmed as disialo-biantennary glycan. And the ion due to monosialo biantennary glycan was observed in MS/MS spectra. The peak at 53 min was collected, and digested with neuraminidase. MS of the obtained asialoglycan showed the molecular ion at  $m/z$  880 as a doubly charged ion (Fig. 1d). MS/MS spectra showed an ion due to chitobiosyl-2AA at  $m/z$  544. These data clearly mean that peak C is due to disialobiantennary glycan. As indicated previously, the automatic apparatus employed for releasing O-glycans does not cleave Asn-GlcNAc linkage, and free N-glycans are not released from the protein core containing Asn-type glycoproteins [10]. This means

that glycan (due to peak C) was endogenously present in serum samples.

To demonstrate if the glycans are due to free glycans in sera, the glycans in sera were directly analyzed after labeling with 2AA. After removing the small-molecular weight materials including glucose and inorganic salts in sera by ultrafiltration and also removing hydrophobic materials using an ODS-cartridge, the eluate (equivalent to 2  $\mu$ L of sera) was analyzed by HPLC after labeling with 2-AA (Fig. 1b). A big peak (peak E) was observed at 53 min, which showed the same elution time with that of peak C observed in Fig. 1a. In addition, the peak showed the same MS and MS/MS profiles with those of peak C (Fig. 1e). In addition, the data also showed well matched results with those of biantennary glycan obtained from transferrin (data not shown). These results indicate that the peak at 53 min was clearly due to the glycan present in sera in free form. It should be noticed that some minor peaks were also observed from 25 min to 65 min.

### 3.2. Detailed analysis of free glycans in a serum sample

As described above, we found that free glycans are present in human serum samples. Fig. 2a shows the results on the detailed

**Table 1**

Summary of free glycans in human serum. (A) before neuraminidase digestion. (B) after neuraminidase digestion.

| Peak no. | <i>m/z</i>   | Monosaccharides composition  | Content of free oligosaccharide (p mol/mL serum) |
|----------|--------------|--|--|
| 1        | (A) 872 (2)  | Hex <sub>4</sub> dHex <sub>1</sub> HexNAc <sub>4</sub> -2AA                    | 175  |
|          | (B) 872 (2)  | Hex <sub>4</sub> dHex <sub>1</sub> HexNAc <sub>4</sub> -2AA                    |  |
| 2        | (A) 953 (2)  | Hex <sub>5</sub> dHex <sub>1</sub> HexNAc <sub>4</sub> -2AA                    | 256  |
|          | (B) 953 (2)  | Hex <sub>5</sub> dHex <sub>1</sub> HexNAc <sub>4</sub> -2AA                    |  |
| 3, 4     | (A) 794 (1)  | NeuAc <sub>1</sub> Hex <sub>1</sub> HexNAc <sub>1</sub> -2AA                   | 264 (peak 3)                                     |
|          | (B) 503 (1)  | Hex <sub>1</sub> HexNAc <sub>1</sub> -2AA                                      | 224 (peak 4)                                     |
| 5        | (A) 1099 (2) | NeuAc <sub>1</sub> Hex <sub>5</sub> dHex <sub>1</sub> HexNAc <sub>4</sub> -2AA | 235  |
|          | (B) 953 (2)  | Hex <sub>5</sub> dHex <sub>1</sub> HexNAc <sub>4</sub> -2AA                    |  |
| 6        | (A) 1025 (2) | NeuAc <sub>1</sub> Hex <sub>5</sub> HexNAc <sub>4</sub> -2AA                   | 844  |
|          | (B) 880 (2)  | Hex <sub>5</sub> HexNAc <sub>4</sub> -2AA                                      |  |
| 7        | (A) 1171 (2) | NeuAc <sub>2</sub> Hex <sub>5</sub> HexNAc <sub>4</sub> -2AA                   | 572  |
|          | (B) 880 (2)  | Hex <sub>5</sub> HexNAc <sub>4</sub> -2AA                                      |  |
| 8        | (A) 1244 (2) | NeuAc <sub>2</sub> Hex <sub>5</sub> dHex <sub>1</sub> HexNAc <sub>4</sub> -2AA | 642  |
|          | (B) 953 (2)  | Hex <sub>5</sub> dHex <sub>1</sub> HexNAc <sub>4</sub> -2AA                    |  |
| 9        | (A) 1171 (2) | NeuAc <sub>2</sub> Hex <sub>5</sub> HexNAc <sub>4</sub> -2AA                   | 7620   |
|          | (B) 880 (2)  | Hex <sub>5</sub> HexNAc <sub>4</sub> -2AA                                      |  |
| 10       | (A) 1070 (2) | NeuAc <sub>2</sub> Hex <sub>5</sub> HexNAc <sub>3</sub> -2AA                   | 235  |
|          | (B) 778 (2)  | Hex <sub>5</sub> HexNAc <sub>3</sub> -2AA                                      |  |
| 11-⊖     | (A) 1048 (3) | NeuAc <sub>3</sub> Hex <sub>6</sub> dHex <sub>1</sub> HexNAc <sub>5</sub> -2AA | 1206<br>(Total contents<br>for 11-⊖ and 11-⊗)    |
|          | (B) 1136 (2) | Hex <sub>6</sub> dHex <sub>1</sub> HexNAc <sub>5</sub> -2AA                    |  |
| 11-⊗     | (A) 999 (3)  | NeuAc <sub>3</sub> Hex <sub>6</sub> HexNAc <sub>5</sub> -2AA                   |  |
|          | (B) 1062 (2) | Hex <sub>6</sub> HexNAc <sub>5</sub> -2AA                                      |  |

dHex, deoxyhexose; Hex, hexose; HexNAc, N-acetyl hexose; NeuAc, N-acetylneuraminic acid.

profile of free glycans present in a serum sample (equivalent to 100  $\mu$ L serum as the injected volume). Each peak was collected and their structures were confirmed by MS technique (Fig. 3 and Table 1). Most of the peaks are commonly found in transferrin and other commercially available samples, and their structures are easily confirmed. Disialylated biantennary glycan showing the molecular ion at *m/z* 1171 (peak 9) as the doubly charged ion was the most abundant glycan as already shown in Fig. 1. The amount was determined to be 7620 pmol/mL of serum as calculated from the fluorescent intensity based on 2-AA residue. Structures of the minor peaks were also determined by MS techniques and comparison of the elution times with those reported previously [9]. At the earlier elution times (ca. 25 min), neutral mono- and di-galactosylated biantennary glycans (1 and 2) were observed. Mono-sialylated biantennary glycans with or without a fucose residue were observed at ca. 39 min (5 and 6). In addition, trisialo-triantennary glycans with or without a fucose residue were also observed at 63 min (11). Interestingly, we found a glycan having a structure of NeuAc-Gal-GalNAc-2AA which is probably due to mucin-type glycoproteins, although the amount of these glycans were only ca. 250 pmol/mL of serum (3 and 4). These peaks (3 and 4) were also assigned by comparison of the elution times with

those reported previously [10]. A characteristic glycan (10), disialo-biantennary glycan having one GlcNAc residue at the reducing end was also present in sera. We previously reported that this glycan was characteristically accumulated in cytosols of stomach tumor cells. The presence of this glycan may indicate that this characteristic glycan is leaked from some organs, although further studies are required [9]. According to the MS observations, peak 7 was assigned as disialo biantennary glycan by MS measurement. This indicates that peak 7 has different linkages of NeuAc to Gal with those of peak 9. Because NeuAc mainly binds to Gal through  $\alpha$ 2-6 linkage in human [20], the glycan (9) is a typical disialo biantennary glycan which has NeuAc $\alpha$ 2-6 linkages. And peak 7 is probably due to disialoglycan which has NeuAc $\alpha$ 2-3 linkages. We also analyzed total N-glycans in a serum sample in order to consider the origin of free glycans in serum in detail. Fig. 2b shows the results on the profile of total N-glycans present in a serum sample (equivalent to 0.75  $\mu$ L serum as the injected volume). As shown in Fig. 2b, the results are quite similar to those in Fig. 2a. It should be emphasized that high mannose-type glycans were not detected at all. This also indicates that these glycans are not due to cells from some organs but from sera, because high mannose-type glycans are major ones found in cytosol fractions through endoplasmic-reticulum associated protein degradation pathway [3].

Sturiale et al. studied glycosylation of transferrin in galactosemia patients in order to figure out hypoglycosylation with increased fucosylation and branching [21]. In the manuscript, they showed N-glycan profiles in a human serum sample (healthy volunteer) examined by MS technique after releasing N-glycans with N-glycoamidase F. The data showed quite similar profiles with those observed in the present study. Namely, Sturiale et al. reported that the ratios of triantennary glycan ((Fuc)Gal<sub>3</sub>GlcNAc<sub>5</sub>Man<sub>3</sub>NeuAc<sub>3</sub>), monosialo-biantennary glycan (Gal<sub>2</sub>GlcNAc<sub>4</sub>Man<sub>3</sub>NeuAc) and disialo-fucosylated biantennary glycan (FucGal<sub>2</sub>GlcNAc<sub>4</sub>Man<sub>3</sub>NeuAc<sub>2</sub>) to the main glycan (Gal<sub>2</sub>GlcNAc<sub>4</sub>Man<sub>3</sub>NeuAc<sub>2</sub>) were 13.5, 9.4 and 6.5%, respectively. In the present study, the ratios of these glycans to the major glycan (9) were 15.8, 11.1 and 8.4%, respectively. These data clearly indicate that these glycans are possibly derived from serum glycoproteins containing transferrin during its circulation in bodies.

Free glycans found in the cytosol have only a single GlcNAc at their reducing termini [2], and this is due to the action of

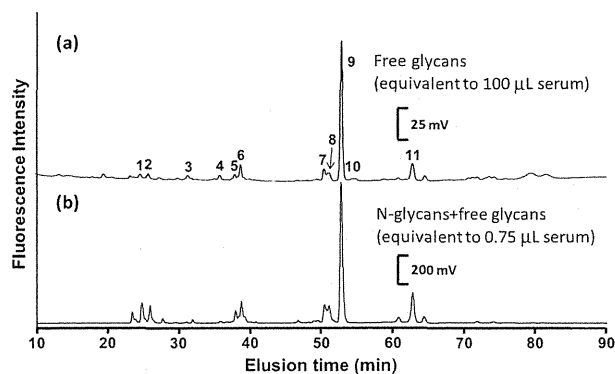


**Fig. 2.** HPLC analysis of (a) free glycans, and (b) total N-glycans in a human serum sample as examined after digestion with N-glycoamidase F. Analytical conditions are the same as those in Fig. 1.

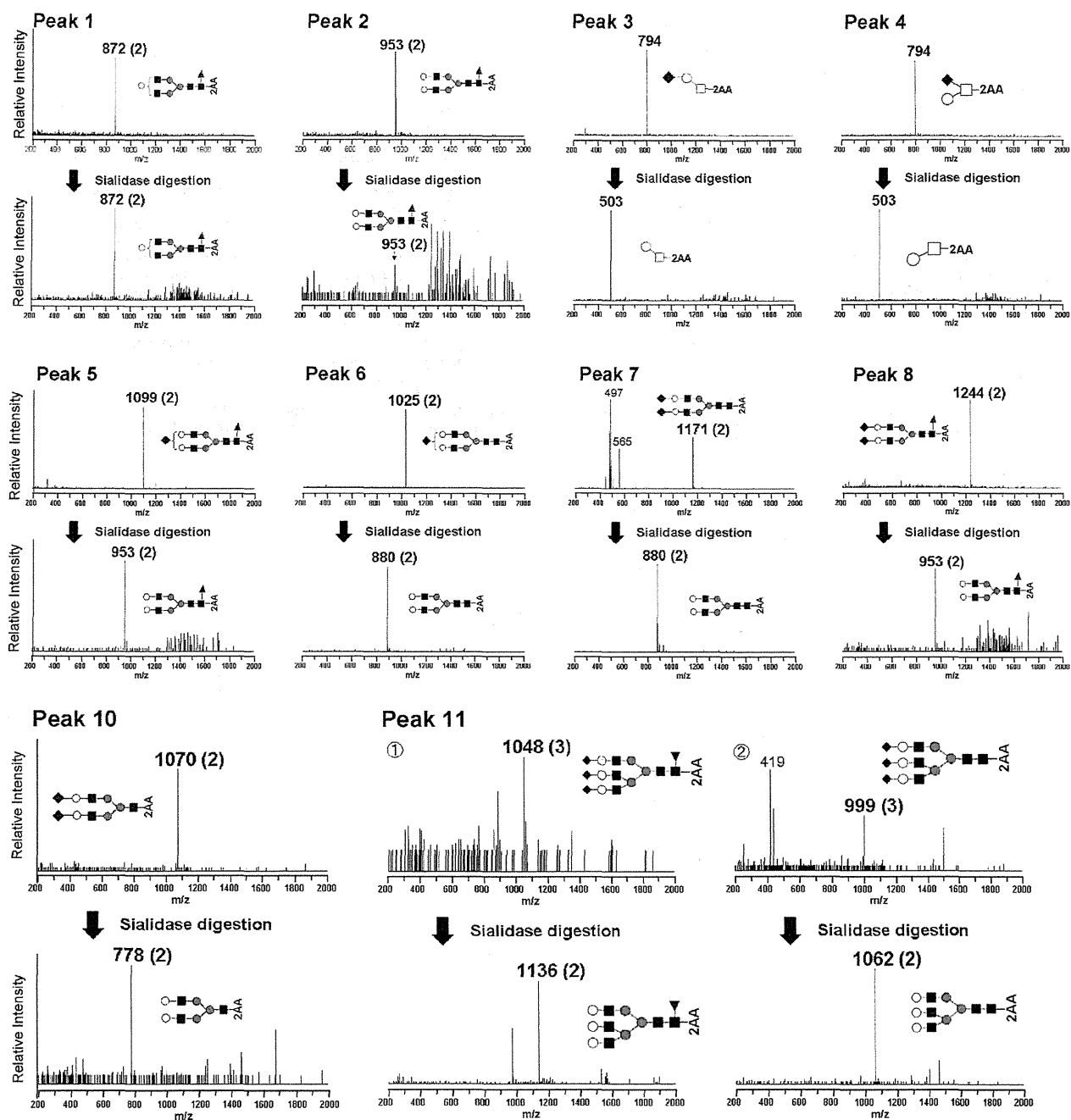


Fig. 3. ESI-IT-TOF mass spectra of peak 1–8, 10, 11 in Fig. 2. Symbols: triangles, fucose; others are the same as those in Fig. 1. Upper panels show the MS spectra of collected peaks. The collected peaks were digested with neuraminidase, and also analyzed by MS (lower panels).

the cytosolic ENGase (endo- $\beta$ -N-acetylglucosaminidase) [22,23] or chitobiase [24]. It should be noted that most free glycans found in the present study bear N-acetylchitobiose structure other than peak 10. Kimura et al. reported that free glycans were accumulated not only inside cells but also secreted to the extracellular space in rice cell culture [25,26]. In addition, they suggested that the extracellular acidic peptide N-glycanase was involved in accumulation of such glycans. We have to also consider the presence of free O-glycans (3 and 4), although the amounts of these glycans are quite small.

The mechanism of the presence/formation of free glycans in sera and the source of these glycans are not clear in the present study. However, it is quite interesting if these glycans are varied with physiological changes.

#### 4. Conclusions

The present study demonstrates that free glycans exist in human serum. Most of the glycans were sialic acid-containing complex-type glycans. Of the glycans, disialo-biantennary glycan which does

not carry fucose residue is present most abundantly. And high mannose-type glycans were not detected at all. From these results, we suppose that these free glycans were due to glycoproteins in sera, although further studies are required.

## References

- [1] D. Kmiecik, V. Herman, C.J. Stoop, A.M. Mir, O. Labiau, A. Verbert, *Glycobiology* 5 (1995) 483.
- [2] K. Yanagida, S. Natsuka, S. Hase, *Glycobiology* 16 (2006) 294.
- [3] T. Suzuki, H. Park, W.J. Lennarz, *FASEB J.* 16 (2002) 635.
- [4] I. Chantret, S.E. Moore, *Glycobiology* 18 (2008) 210.
- [5] T. Suzuki, Y. Funakoshi, *Glycoconj. J.* 23 (2006) 291.
- [6] D.J. Kelleher, R. Gilmore, *Glycobiology* 16 (2006) 47R.
- [7] T. Suzuki, *Semin Cell, Dev. Biol.* 18 (2007) 762.
- [8] R. Naka, S. Kamoda, A. Ishizuka, M. Kinoshita, K. Takechi, *J. Proteome Res.* 5 (2006) 88.
- [9] A. Ishizuka, Y. Hashimoto, R. Naka, M. Kinoshita, K. Takechi, J. Seino, *Biochem. J.* 413 (2008) 227.
- [10] Y. Matsuno, K. Yamada, A. Tanabe, M. Kinoshita, S. Maruyama, Y. Osaka, T. Masuko, K. Takechi, *Anal. Biochem.* 362 (2007) 245.
- [11] K. Yamada, S. Hyodo, Y. Matsuno, M. Kinoshita, S. Maruyama, Y. Osaka, E. Casal, Y.C. Lee, K. Takechi, *Anal. Biochem.* 371 (2007) 52.
- [12] K. Yamada, M. Kinoshita, T. Hayakawa, S. Nakaya, K. Takechi, *J. Proteome Res.* 8 (2009) 521.
- [13] K. Yamada, S. Hyodo, M. Kinoshita, T. Hayakawa, K. Takechi, *Anal. Chem.* 82 (2010) 7436.
- [14] B. Winchester, *Glycobiology* 15 (2005) 1R.
- [15] J.C. Michalski, J. Lemone, J.M. Wieruszkeski, B. Fournet, J. Montreuil, G. Strecker, *Eur. J. Biochem.* 198 (1991) 521.
- [16] G. Strecker, M.C. Peers, J.C. Michalski, T. Hon-di-Assah, B. Fournet, G. Spik, J. Montreuil, J.P. Farriaux, P. Maroteaux, P. Durand, *Eur. J. Biochem.* 75 (1977) 391.
- [17] J. van Pelt, K. Hard, J.P. Kamerling, J.F. Vliegthart, A.J. Reuser, H. Galjaard, *Biol. Chem. Hoppe-Seyler* 370 (1989) 191.
- [18] K. Ishii, M. Iwasaki, S. Inoue, P.T.M. Kenny, H. Komura, Y. Inoue, *J. Biol. Chem.* 264 (1989) 1623.
- [19] M. Tajiri, C. Ohyama, Y. Wada, *Glycobiology* 18 (2008) 2.
- [20] G. Weisshaar, J. Hiyama, A.G.C. Renwick, *Glycobiology* 1 (1991) 393.
- [21] L. Sturiale, R. Barone, A. Fiumara, M. Perez, M. Zaffanello, G. Sorge, L. Pavone, S. Tortorelli, J.F. O'Brien, J. Jaeken, D. Garozzo, *Glycobiology* 15 (2005) 1268.
- [22] T. Kato, K. Hatanaka, T. Mega, S. Hase, *J. Biochem.* 122 (1997) 1167.
- [23] T. Suzuki, K. Yano, S. Sugimoto, K. Kitajima, W.J. Lennarz, S. Inoue, Y. Inoue, Y. Emori, *Proc. Natl. Acad. Sci. U.S.A.* 99 (2002) 9691.
- [24] R. Cacan, C. Dengremont, O. Labiau, D. Kmiecik, A. Mir, A.M. Verbert, *J. Biochem.* 313 (1996) 597.
- [25] Y. Kimura, S. Matsuo, *J. Biochem.* 127 (2000) 1013.
- [26] M. Maeda, M. Kimura, Y. Kimura, *J. Biochem.* 148 (2010) 681.



Masahiro Yodoshi  
Natsumi Ikeda  
Naoko Yamaguchi  
Mana Nagata  
Noriaki Nishida  
Kazuaki Kakehi  
Takao Hayakawa  
Shigeo Suzuki

Faculty of Pharmaceutical  
Sciences, Kinki University,  
Kowakae, Higashi-Osaka, Osaka,  
Japan

Received November 13, 2012  
Revised September 2, 2013  
Accepted September 5, 2013

## Research Article

# A novel condition for capillary electrophoretic analysis of reductively aminated saccharides without removal of excess reagents

We have identified novel CE conditions for the separation of 7-amino-4-methylcoumarin-labeled monosaccharides and oligosaccharides from glycoproteins. Using a neutrally coated capillary and alkaline borate buffer containing hydroxypropylcellulose and ACN, saccharide derivatives form anionic borate complexes, which move from the cathode to the anode in an electric field and are detected near the anodic end. Excess labeling reagents and other fluorescent products remain at the cathodic end. Fluorimetric detection using an LED as a light source enables determination of monosaccharide derivatives with good linearity between at least 0.4 and 400  $\mu\text{M}$ , may correspond to 140 amol to 140 fmol. The lower LOD ( $S/N = 5$ ) is only 80 nM in the sample solution (ca. 28 amol). The results were comparable to reported values using fluorometric detection LC. The method was also applied to the analysis of oligosaccharides that were enzymatically released from glycoproteins. Fine resolution enables profiling of glycans in glycoproteins. The applicability of the method was examined by applying it to other derivatives labeled with nonacidic tags such as ethyl *p*-aminobenzoate- and 2-aminoacridone-labeled saccharides.

### Keywords:

7-Amino-4-methylcoumarin / Borate complex / Glycoprotein glycans / Monosaccharide analysis / Reductive amination  
DOI 10.1002/elps.201200612

## 1 Introduction

Most saccharides are neutral, highly hydrophilic, and do not possess chromophoric or fluorometric functions. Various labeling reagents have therefore been developed to improve sensitivity and enhance resolution in LC and CE. Numerous fluorescent amines have been reported for the derivatization of saccharides based on reductive amination. In this labeling reaction, a saccharide is converted to a Schiff's base in the presence of a large excess of an aromatic amine and the resultant imide derivative is converted immediately to a chemically stable 1-amino-1-alditol by reduction with sodium cyanoborohydride. These reactions are well summarized in a number of reviews [1–3]. 8-Aminopyrene-1,3,6-trisulfonic

acid (APTS) is often used for sensitive detection of glycoprotein glycans in CE analysis because APTS derivatives show intense fluorescence signals under irradiation by an argon ion laser. The negative charge attributable to the three sulfonate groups of APTS moves derivatized saccharides to the anode at high velocity, which enables the rapid analysis of glycoprotein glycans [4–8]. 2-Aminopyridine is often used for identification of glycoprotein-derived oligosaccharides because retention indices for more than several hundred glycans have been accumulated in RP and normal phase LC, as well as anion-exchange LC for sialylated oligosaccharides [9–13]. However, the high hydrophilicity of APTS and 2-aminopyridine hampers solvent extraction of excess reagents. Therefore, tedious steps are required to remove excess reagents from the reaction mixture. Moreover this process may cause partial loss of derivatives, which impairs quantitative analysis.

We previously described a labeling method using 7-amino-4-methylcoumarin (AMC) as a fluorescent probe [14]. AMC-labeled oligosaccharides displayed one- to two-order higher intensities in ESI-MS than derivatives labeled with other reagents. However the method requires two-step SPE for the removal of excess AMC and by-products generated in the course of reaction, which requires tedious procedures and may partially impair quantitative determination.

**Correspondence:** Dr. Shigeo Suzuki, Faculty of Pharmaceutical Sciences, Kinki University in 3-4-1, Kowakae, Higashi-Osaka, Osaka, Japan

**E-mail:** suzuki@phar.kindai.ac.jp

**Fax:** +81-6-6721-2353

**Abbreviations:** ABEE, ethyl *p*-aminobenzoate; AMAC, 2-aminoacridone; AMC, 7-amino-4-methylcoumarin; APTS, 8-aminopyrene-1,3,6-trisulfonic acid; BSM, bovine submaxillary mucin; Fuc, fucose; Gal, galactose; GalNAc, *N*-acetylgalactosamine; GlcNAc, *N*-acetylglucosamine; IS, internal standard; Man, mannose; ManNAc, *N*-acetylmannosamine; NeuAc, *N*-acetylneuraminic acid; NeuGc, *N*-glycolylneuraminic acid; Rha, rhamnose; Xyl, xylose

Colour Online: See the article online to view Fig. 5 in colour.

This work presents selective and sensitive separation conditions for profiling monosaccharides and oligosaccharides found in glycoproteins, without requiring the two-step extractive removal of excess labeling reagent. AMC-labeled saccharides have no charge in alkaline buffer. However in the presence of boric acid, the adjacent hydroxyl groups on saccharides form acidic complexes with borate, which provide a strong negative charge to AMC-labeled saccharides and induces their movement toward the anode. This method allows selective quantification of all of component monosaccharides found in glycoprotein hydrolysates; *N*-acetylglucosamine (GlcNAc), *N*-acetylgalactosamine (GalNAc), galactose (Gal), mannose (Man), fucose (Fuc), *N*-acetylneuraminic acid (NeuAc), and *N*-glycolylneuraminic acid (NeuGc). Application of LED-based fluorescent detection enables subattomole level detection of monosaccharides. This borate-based separation mode was also applied to the selective detection of glycoprotein-derived oligosaccharides.

## 2 Materials and methods

### 2.1 Materials

We obtained AMC from Tokyo Kasei Kogyo Co. (Tokyo, Japan). Pyridine-borane, DMF, ethyl *p*-aminobenzoate (ABEE), ACN, methanol, TFA, and glacial acetic acid were obtained from Wako Pure Chemical Industries (Doshomachi, Osaka, Japan).  $\beta$ -*N*-Acetylhexosaminidase (jack bean, EC 3.2.1.52) and  $\beta$ -galactosidase (jack bean, EC 3.2.1.23) were obtained from Seikagaku Kogyo K.K. (Tokyo, Japan). Dimethylamine-borane complex, 2-aminoacridone (AMAC), *N*-acetylneuraminic pyruvate-lyase from *Escherichia coli* K-12, human transferrin, fetal calf serum fetuin, bovine pancreas ribonuclease B, human  $\alpha_1$ -acid glycoprotein, bovine submaxillary mucin (BSM), and ovalbumin were obtained from Sigma-Aldrich Japan K.K. (Tokyo, Japan). Neuraminidase from *Arthrobacter ureafaciens* and saccharide specimens were obtained from Nacalai Tesque (Kyoto, Japan). Peptide-*N*<sup>4</sup>-(acetyl- $\beta$ -glucosaminyl)-asparagine amidase F (EC 3.5.1.52) was purchased from F. Hoffmann-La Roche (Mannheim, Germany). Isomaltooligosaccharides were obtained through partial hydrolysis of dextran (100 mg) with 1 mL of 0.1 M hydrochloric acid for 4 h at 100°C; the lyophilized powder was used as a glucose ladder. Water was purified using a Milli-Q device (Millipore, Milford, MA, USA). Other reagents and solvents were of the highest commercially available grade. In addition, SCX-type SPE cartridges (100 mg) and OASIS HLB cartridges (10 mg) were obtained from Silicycle (Quebec, Canada) and Nihon Waters K.K. (Tokyo, Japan), respectively. Graphitized carbon was from Alltech Japan (Tokyo, Japan). AMC-labeled maltose was prepared as described in a previous report, and AMC-labeled oligosaccharides derived from glycoprotein specimens were fractionated by HPLC and used for peak identifications [14].

### 2.2 Hydrolysis of glycoprotein specimens

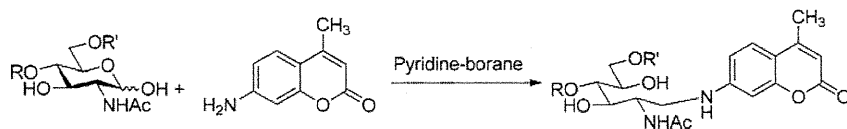
Hydrolysis of glycoprotein specimens was carried out as previously described [15]. Two portions of a solution of glycoprotein specimen (0.1 mg each) were lyophilized in glass tubes (4 mm id, 12 cm long). For the analysis of component neutral aldoses, one of the sample residues was dissolved in 100  $\mu$ L of 2 M TFA and the tube was sealed after exchanging air in the tube with nitrogen three times using a vacuum desiccator connected to nitrogen and vacuum lines, and the tube was then sealed and heated for 6 h at 100°C. The resultant solution was mixed with 20  $\mu$ L of 0.1 mM rhamnose (Rha, 2 nmol) as internal standard (IS), and the residue was lyophilized to dryness for derivatization with AMC. For the analysis of hexosamines, a sample was dissolved in 100  $\mu$ L of 4 M HCl and the solution was heated for 6 h at 100°C under a nitrogen atmosphere. The solution was then evaporated to dryness, followed by addition of 2 nmol IS. Acetamide groups were hydrolyzed in this process. Therefore the residue was dissolved in 250  $\mu$ L of a saturated solution of sodium bicarbonate and the solution mixed with 50  $\mu$ L of acetic anhydride under vigorous shaking for 30 min and stored in a refrigerator overnight. The reaction mixture was mixed with 500  $\mu$ L of water and DI by passing through a column containing 1 mL of Amberlite CG120 (H<sup>+</sup> form) resin, and the column was then washed with 5 mL of water. The combined eluate and washing fluids were evaporated to dryness and derivatized with AMC. For the analysis of sialic acids, a glycoprotein sample was dissolved in 100  $\mu$ L of 60 mM phosphate buffer (pH 7.0) containing neuraminidase (0.1 U) and *N*-acetylneuraminic pyruvate-lyase (0.1 U), and the mixture was incubated for 5 h at 37°C. After the mixture was heated for 1 min at 100°C, the solution was DI with a column containing 1 mL each of Amberlite CG120 (H<sup>+</sup> form) and CG400 (acetate form) resins, followed by addition of 2 nmol IS.

### 2.3 Preparation of oligosaccharides from glycoproteins

*N*-Linked oligosaccharides were prepared from 50  $\mu$ g of each lyophilized glycoprotein. Each sample was dissolved in 50  $\mu$ L of 50 mM phosphate buffer (pH 7.9) containing 0.1% SDS and 2% 2-mercaptoethanol. The solution was heated at 100°C for 5 min. After cooling, the solution was mixed with 5  $\mu$ L of 7.5% NP-40 and 5 mU of peptide-*N*<sup>4</sup>-(acetyl- $\beta$ -glucosaminyl)-asparagine amidase F, and the reaction mixture incubated for 2 h at 37°C. Deglycosylated proteins were precipitated by the addition of 180  $\mu$ L of ice-cold ethanol and removed by centrifugation at 10 000 rpm for 5 min. The supernatant was dried using a centrifugal evaporator (Tomy, Tokyo, Japan) and stored in a refrigerator until use.

### 2.4 Derivatization of saccharides with AMC

Scheme 1 shows the reductive amination reaction of saccharides with AMC. The procedure was described previously [14].



**Scheme 1.** Reductive amination of a saccharide with AMC as a fluorescent tag.

Briefly, a lyophilized sample containing saccharides (~10 nmol) in a screw-capped polypropylene tube (0.5 mL volume) was mixed with 20  $\mu\text{L}$  of AMC solution (60 mM in DMF) and then mixed with 20  $\mu\text{L}$  of pyridine–borane solution (0.2 M in acetic acid). The solution was then heated at 70°C for 60 min and the reaction terminated by addition of 60  $\mu\text{L}$  of water and chilling of the reaction mixture in an ice bath, followed by evaporation to dryness. The resultant residues were dissolved in 500  $\mu\text{L}$  of 0.5 M acetic acid in aqueous 30% ACN for CE analysis.

## 2.5 Derivatization of saccharides with AMAC and ABEE

A monosaccharide mixture or isomaltooligosaccharides was labeled according to previously reported methods [16, 17] with slight modification. Each 2.5  $\mu\text{L}$  of 0.3 M AMAC in DMSO/30% acetic acid (7:3, v/v), and 1 M  $\text{NaBH}_3\text{CN}$  in DMSO was added to dry saccharide samples (~10 nmol). The solution was incubated at 37°C overnight and the reaction terminated by adding 50  $\mu\text{L}$  of water–methanol (1:1, v/v).

A 20  $\mu\text{L}$  portion of ABEE solution (1 mmol of ABEE and 35 mg of  $\text{NaBH}_3\text{CN}$ , and 41  $\mu\text{L}$  of acetic acid dissolved in 350  $\mu\text{L}$  of methanol) was added to a saccharide sample (~100 nmole), and the solution was heated at 80°C for 1 h. The resultant solution was dried and dissolved in 100  $\mu\text{L}$  of water–methanol (9:1, v/v). Excess ABEE, immiscible in the solvent, was removed by centrifugation, and the supernatant was used for the CE analysis.

## 2.6 Instrumentation for CE analysis

Apart from a reference experiment using a bare fused silica capillary (50  $\mu\text{m}$  id) for Fig. 1A, PDMS-coated capillaries (InertCap I<sup>®</sup>; GL Sciences, Tokyo, Japan) of 50  $\mu\text{m}$  id with an effective length of 40 cm (50 cm in total) were used, with a 1:9, v/v, mixture of ACN and borate buffer containing 0.05% hydroxypropylcellulose as a BGE; 200 mM sodium borate (pH 9.5) for monosaccharide analysis and 250 mM potassium borate (pH 9.0), and 100 mM Tris borate (pH 8.5) for neutral and acidic oligosaccharide separation, respectively. A P/ACE MDQ CE system (Beckman Coulter, Brea, CA, USA) was used. An LED light (LLS-365, Ocean Photonics) as a source of 365 nm light was connected with an optical fiber (P600-2-UV/Vis, Ocean Photonics), and the fluorescence due to AMC derivatives was detected by passing through a 420 nm band path filter. The capillary was thermostated at 25°C. Sample

solution was injected for 5 s by application of pressure of 3.45 kPa. Separation was conducted by application of –15 kV. After each run, the capillary was washed by introducing a buffer solution from the outlet of the capillary using pressure (34.5 kPa, 2 min). AMAC derivatives were detected fluorometrically using an argon laser (488 nm) and the optical system for the fluorescein detection. ABEE derivatives were detected based on absorbance at 312 nm. Other conditions were the same as those for AMC derivatives.

The volume of sample solution injected into the capillary was not certain. Here we chose the following calculation to estimate injected amount of sample in sample solution:

$$V = \frac{\Delta P d^4 \pi t}{128 \eta L}$$

where  $V$  is the volume in  $\text{m}^3$  delivered across the capillary,  $\Delta P$  denotes the pressure drop across the capillary (Pa),  $d$  signifies the internal diameter of the capillary (m),  $t$  is the duration of pressure application (s),  $\eta$  represents the buffer viscosity (Pa·s), and  $L$  is the total capillary length (m).

## 3 Results and discussion

### 3.1 Optimization of separation conditions

Alkaline borate buffer has often been used in CE separation of mixtures of monosaccharide derivatives [18]. Borate forms complexes with polyalcohols, including saccharide derivatives in solution, and the borate–polyalcohol complexes possess negative charges, which are forced to move toward the anode in an electric field. Stability and negativity of the saccharide–borate complex depend on the configuration of adjacent hydroxyl groups (i.e., the type of monosaccharide). Moreover, the pH and concentration of borate buffer influence the formation of polyoxy acid with borate ions as well as the complex formation, and therefore also affect the mobility of borate–polyol complexes [19]. Most reports on CE of monosaccharide derivatives using alkaline borate buffer were performed using a bare fused silica capillary. Under such conditions, monosaccharide derivatives travel from anode to cathode because of strong EOF, and separate as anions, based on the molecular size and stability of the borate complexes. Moreover, a large amount of excess fluorescent reagents also travels to the cathode, which may cause deviations in migration times and heavy drift of baselines.

Here, we used a PDMS-coated capillary instead of a bare fused silica capillary to suppress EOF and to specifically move acidic borate–saccharide complexes toward the anode. Reductive amination of carbohydrates with primary amines generates secondary amine derivatives of linear polyalcohols (i.e.,

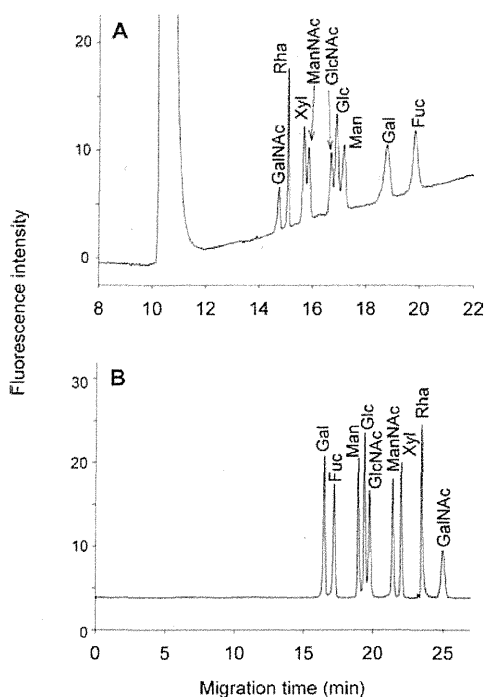


**Figure 1.** Fluorescent CE analysis of selected monosaccharides in borate complexation mode using a bare fused silica capillary (A) and a PDMS-coated capillary (B). Analytical conditions: BGE, ACN and 200 mM sodium borate (pH 9.5) containing 0.05% hydroxypropylcellulose (1:9, v/v); capillary size, 50  $\mu\text{m}$  id  $\times$  50 cm (40 cm for detector); capillary temperature, 25°C; applied voltage +15 kV (A) and –15 kV (B); detection, fluorescence with 365 nm LED.

aminoalditols). Excess aromatic amines and their decomposition products residing in the reaction mixture cannot be charged in alkaline borate buffer. In contrast, monosaccharide derivatives having linear polyalcohol structures easily generate negative charges as borate complexes, which move toward the anode in an electric field. Therefore, the excess reagents in the reaction mixture can be removed from electropherograms without requiring purification before analysis.

Figure 1A shows the separation of AMC derivatives of monosaccharides obtained by reaction on positive mode separation using a bare capillary and alkaline borate buffer as BGE. Reaction products of AMC-labeled derivatives show an intense, tailing signal of excess AMC at 11 min and baseline drift, which could not be removed by addition of surfactants to the BGEs. In contrast, a combination of negative separation mode using 200 mM borate buffer containing 0.05% hydroxypropylcellulose and PDMS-coated capillary, as shown in Fig. 1B, suppressed the generation of EOF and therefore induced the movement of anionic borate complexes to the anode. This enables specific detection of saccharide derivatives. Addition of ACN prevents the precipitation of excess reagent. Therefore, the electropherogram comprised peaks corresponding to monosaccharide derivatives, with no peaks

because of excess reagent. This result indicates the usefulness of the separation conditions.

### 3.2 Monosaccharide analysis

We previously reported that the use of pyridine-borane rather than the sodium cyanoborohydride normally used enables quantitative derivatization of all component monosaccharides in glycoproteins [14]. Here, we optimized the separation conditions of AMC-labeled monosaccharides containing excess reagents using CE with fluorometric detection by LED.

The resolution between AMC monosaccharide derivatives depends strongly on the pH of the borate buffer and also the species and concentration of organic solvent. Resolution of Man-Glc-GlcNAc and ManNAc-Xyl is invariant with pH but the separation window (i.e., time window for separation of monosaccharides) is broadened with increasing electrophoresis buffer pH. The concentration of the borate buffer mainly affects the peak shape of AMC derivatives. With increasing buffer concentration, the sharpness of AMC monosaccharide peaks increased, reaching a maximum of over 200 mM. The higher concentration causes Joule heating because of the increase in electric current. Addition of a water-miscible solvent such as methanol, ethanol, or ACN is essential to prepare a clear solution from the AMC reaction mixture because of the low solubility of AMC in water. Among these three solvents, we found that the addition of ACN enhanced the resolution of fucose from other monosaccharide derivatives. Baseline resolution was obtained using a 1:9 v/v mixture of ACN and borate buffer containing 0.05% hydroxypropylcellulose. However, the anions residing in the reaction mixture partly diminished the sharpness of specific peaks. To enhance the sharpness of saccharide peaks, acetic acid was added to AMC-labeled sample at a concentration of 0.5 M. Good resolution between the nine monosaccharide derivatives was obtained under the optimized conditions, as shown in Fig. 1B.

### 3.3 Analysis of component monosaccharides in glycoproteins

The optimized conditions were applied to the analysis of component monosaccharides in a number of glycoproteins. Saccharide chains in glycoproteins comprise Man, Gal, Fuc, GlcNAc, GalNAc, NeuAc, and NeuGc. Before the analysis, the linearity range and lower LOD were examined. As shown in Fig. 2, linear quantitation ranges were obtained over the concentration range between at least 0.4 and 400  $\mu\text{M}$  (calculated to be 140 amol to 140 fmol). Figure 3 shows the separation of 4, 0.4, and 0.04  $\mu\text{M}$  mixture. Apparently, 4 and 0.4  $\mu\text{M}$  are within the quantitation range, but the concentration of 0.04  $\mu\text{M}$  were apparently below the detection limit, for example, peak height of Rha is only 2.5 times of noise. Therefore we determined 80 nM (ca. 28 amol) as the LOD ( $S/N = 5$ ). The hydrolytic conditions required for quantitative